

Actin binding to WH2 domains regulates nuclear import of the multifunctional actin regulator JMY

J. Bradley Zuchero, Brittany Belin, and R. Dyche Mullins

Cellular and Molecular Pharmacology, University of California, San Francisco, San Francisco, CA 94158; Physiology Course, Marine Biological Laboratory, Woods Hole, MA 02543

ABSTRACT Junction-mediating and regulatory protein (JMY) is a regulator of both transcription and actin filament assembly. In response to DNA damage, JMY accumulates in the nucleus and promotes p53-dependent apoptosis. JMY's actin-regulatory activity relies on a cluster of three actin-binding Wiskott–Aldrich syndrome protein homology 2 (WH2) domains that nucleate filaments directly and also promote nucleation activity of the Arp2/3 complex. In addition to these activities, we find that the WH2 cluster overlaps an atypical, bipartite nuclear localization sequence (NLS) and controls JMY's subcellular localization. Actin monomers bound to the WH2 domains block binding of importins to the NLS and prevent nuclear import of JMY. Mutations that impair actin binding, or cellular perturbations that induce actin filament assembly and decrease the concentration of monomeric actin in the cytoplasm, cause JMY to accumulate in the nucleus. DNA damage induces both cytoplasmic actin polymerization and nuclear import of JMY, and we find that damage-induced nuclear localization of JMY requires both the WH2/NLS region and importin β . On the basis of our results, we propose that actin assembly regulates nuclear import of JMY in response to DNA damage.

Monitoring Editor

Thomas D. Pollard
Yale University

Received: Dec 3, 2011

Revised: Jan 6, 2012

Accepted: Jan 9, 2012

INTRODUCTION

Junction-mediating and regulatory protein (JMY) leads a double life in vertebrate cells. In the cytoplasm it promotes actin filament assembly and contributes to cell migration (Zuchero et al., 2009), whereas in the nucleus it acts as a transcriptional coactivator and promotes programmed cell death in response to DNA damage (Shikama et al., 1999; Coutts et al., 2007). The connection between these distinct cellular functions has remained mysterious.

JMY's effects on actin assembly require its C-terminal WWWCA region, composed of three, tandem actin monomer-binding sequences (Wiskott–Aldrich syndrome protein homology 2 [WH2] domains) and an Arp2/3-binding central and acidic (CA) region. Similar

to WH2-CA domains found in Wiskott–Aldrich syndrome protein–family proteins, this region of JMY can promote actin nucleation by the Arp2/3 complex (Welch and Mullins, 2002). In addition, the cluster of WH2 domains can also nucleate actin filaments by itself, using a mechanism remarkably similar to that of the spire–family proteins (Quinlan et al., 2005). In slow-moving cells (e.g., fibroblasts) endogenous JMY occurs in both the nucleus and the cytoplasm, but in highly motile cells (e.g., neutrophils), it is predominantly cytoplasmic and specifically enriched at the leading edge. Both the rate of cell migration and the cytoplasmic concentration of filamentous actin increase when JMY is overexpressed and decrease when JMY expression is knocked down by RNA interference (RNAi; Zuchero et al., 2009). The JMY-dependent increase in cell motility requires its Arp2/3-binding region and is not observed when JMY localization is restricted to the nucleus (Coutts et al., 2009; Zuchero et al., 2009) either by DNA damage or by fusion to a strong nuclear localization sequence (NLS). In nerve cells, JMY appears to suppress neurite outgrowth, an activity that requires its intrinsic actin nucleation activity (Firat-Karalar et al., 2011). Of interest, actin assembly by the Arp2/3 complex also suppresses neurite outgrowth and axon migration in nerve cells (Strasser et al., 2004). Taken together, the data indicate that JMY regulates cell shape and motility, at least in part, by promoting actin assembly in the cytoplasm.

This article was published online ahead of print in MBoC in Press (<http://www.molbiolcell.org/cgi/doi/10.1091/mbc.E11-12-0992>) on January 19, 2012.

Address correspondence to: R. Dyche Mullins (dyche@mullinslab.ucsf.edu).

Abbreviations used: ABD, actin-binding domain; Imp α , importin α ; Imp β , importin β ; jasp, jasplakinolide; JMY, junction-mediating and regulatory protein; LatB, latrunculin B; LMB, leptomycin B; NLS, nuclear localization signal; WH2, Wiskott–Aldrich syndrome protein homology 2 domain.

© 2012 Zuchero et al. This article is distributed by The American Society for Cell Biology under license from the author(s). Two months after publication it is available to the public under an Attribution–Noncommercial–Share Alike 3.0 Unported Creative Commons License (<http://creativecommons.org/licenses/by-nc-sa/3.0/>).

"ASCB®," "The American Society for Cell Biology®," and "Molecular Biology of the Cell®" are registered trademarks of The American Society of Cell Biology.

In response to DNA damage, JMY accumulates in the nucleus, where it enhances transcription by the tumor suppressor p53 and promotes apoptosis (Shikama et al., 1999; Coutts et al., 2007). Three additional proteins are known to modulate JMY's nuclear function: the acetyltransferase p300, an adaptor protein called Strap, and the ubiquitin ligase Mdm2. In the nucleus, JMY forms a complex with p300 and Strap that is believed to acetylate p53 and increase its proapoptotic transcriptional activity. Mdm2 can oppose this activity by promoting degradation of both JMY and p53. Given growing evidence that actin has important functions in the nucleus, including regulation of transcription, it is tempting to speculate that JMY might make actin filaments in the nucleus. There is, however, no evidence to support this idea.

To understand the connection between its nuclear and cytoplasmic functions, we investigated the mechanism by which JMY translocates from the cytoplasm into the nucleus. Surprisingly, we find that decreases in the cytoplasmic concentration of monomeric actin drive translocation of JMY into the nucleus and that actin-dependent translocation is controlled by the cluster of WH2 domains. We identified a bipartite nuclear localization sequence that partially overlaps the WH2 cluster and found that WH2 mutations that prevent actin binding are sufficient to drive JMY into the nucleus. *In vitro*, monomeric actin bound to the WH2 domains blocks access of the importin α/β (Imp α/β) complex to JMY's NLS. This mechanism of regulation is remarkably similar to that of the myocardin-related transcription factor (MRTF) proteins, whose nuclear localization is also actin dependent but which use an unrelated actin-binding sequence called a RPEL domain. The lack of sequence similarity and the evolutionary history of JMY argue strongly that the similarities in MRTF and JMY regulation represent a case of convergent evolution. Of interest, DNA damage-induced nuclear accumulation of JMY absolutely requires the actin-sensitive nuclear localization sequence embedded in the WWWCA domain. We find that DNA damage sufficient to produce nuclear accumulation of JMY also induces incorporation of monomeric actin into cytoplasmic filaments incapable of binding JMY. Our work argues strongly that nuclear translocation of JMY in response to DNA damage is an actin-dependent process.

RESULTS

Identification of proteins with both a putative actin-binding domain and NLS

To identify factors that might link actin dynamics to nuclear events, we searched the human genome for coding sequences containing one or more potential actin-binding domains and at least one predicted nuclear localization sequence (Nair et al., 2003). We tested both actin monomer-binding (WH2 and RPEL) and filament-binding (calponin homology, formin homology 2, ILWEQ, and ezrin/radixin/moesin) sequences and identified 28 proteins that met our criteria (Supplemental Table S1). Of interest, in 14 of these proteins the predicted actin-binding domain (ABD) overlaps or is adjacent to the NLS (Figure 1A). This motif occurs in several well-known actin monomer-binding proteins (JMY, MRTF proteins, Phactr1-4, Scar2/WAVE2), formin-family members (Daam1-2, Diaph1, Fhod3), canonical adhesion proteins (ezrin, radixin, moesin, talin), and others, including SYNE/nesprin proteins, dystonin, neuron navigator, and huntingtin interacting protein 1.

We used cell fractionation and fluorescence microscopy to test whether the proteins with overlapping ABD and NLS sequences shuttle between the cytoplasm and nucleus and whether their localization depends on the state of the actin cytoskeleton. We treated cells with jasplakinolide (jasp) to polymerize actin and reduce the cytoplasmic concentration of actin monomers (Bubb et al., 1994,

2000; Kiuchi et al., 2011), latrunculin B (LatB) to depolymerize actin filaments and increase monomer concentration (Spector et al., 1983; Lyubimova et al., 1997), or leptomycin B (LMB) to inhibit exportin1/Crm1-dependent nuclear export (Wolff et al., 1997). We then fractionated cells into cytoplasmic and nuclear pools and assessed protein localization by immunoblotting (Supplemental Figure S1A). Probes against cytoplasmic (HSP70) and nuclear (lamin B1) markers demonstrate the efficiency of fractionation (Figure 1B and Supplemental Figure S1A). When suitable antibodies were not available, we expressed candidates as green fluorescent protein (GFP) fusions (including MAL and Phactr1) and analyzed localization by fluorescence microscopy (Supplemental Figure S1B).

Actin regulates the subcellular localization of JMY

Of the 14 proteins we tested, only three exhibit changes in localization as a function of actin assembly/disassembly: JMY, MAL (also known as MRTF-A and MKL1), and Phactr1. Consistent with previous reports (Vartiainen et al., 2007), MAL accumulates in the nucleus in response to jasp and LMB and in the cytoplasm in response to LatB (Supplemental Figure S1B, top). Phactr1, another RPEL motif-containing protein (Sagara et al., 2009), accumulates in the nucleus in response to jasp (Supplemental Figure S1B, bottom, and c) and colocalizes with actin-based structures in the cytoplasm (Supplemental Figure S1D). It is striking that both endogenous and GFP-tagged JMY also accumulate in the nucleus in response to jasp (fold increase in nuclear JMY, 2.45 ± 0.62 SEM; in GFP-JMY, 2.68 ± 0.14 ; Figure 1, B and C, and Supplemental Figure S1A). We confirmed these results by fluorescence microscopy of GFP-JMY in live cells (Figure 1, D and E). GFP-JMY was enriched in the nucleus of only $2.2 \pm 1.1\%$ of mock-treated cells ($78.6 \pm 5.4\%$ predominantly cytoplasmic), and treatment with jasp increased this localization by almost 10-fold ($19.0 \pm 2.4\%$ nuclear; $31.3 \pm 2.7\%$ cytoplasmic). In contrast to MAL, however, we observed no change in JMY localization in response to LMB or LatB (Supplemental Figure S1A; see also later discussion of Figure 3).

Does the actin-dependent localization of JMY depend on its ability to bind actin monomers? To test this, we made point mutations in JMY WH2 domains (where [A*B*C*] refers to mutations made in WH2-a, -b, and -c) previously shown to compromise actin binding (Quinlan et al., 2005; Kelly et al., 2006). We validated these mutations *in vitro* using pyrene actin assembly assays (Supplemental Figure S2, A and B). Consistent with the effects of jasp, compromising the ability of all three WH2 domains to bind actin (GFP-JMY[A*B*C*]) causes JMY to become completely nuclear (Figure 1F). Putative NLS-2 overlaps both the C-terminal LRKT motif of WH2-a and the linker connecting it to WH2-b (Supplemental Figure S2C), and so we tested the effect of mutating only the first two WH2 domains. Similar to the [A*B*C*] triple mutant, the double mutant GFP-JMY[A*B*] also accumulates in the nucleus despite being able to bind actin on WH2-c (Figure 1F and Supplemental Figure S2, A and B). These results suggest that actin monomers bound to WH2-a and -b block JMY nuclear import by masking NLS-2.

To understand the function and regulation of JMY's putative NLS regions, we tested their function by fusing them to GFP. The nuclear pore complex has a mesh size of ~2.6 nm and, in the absence of a functional NLS, GFP (Stokes radius, 2.4 nm) equilibrates slowly between the nucleus and cytoplasm (Mohr et al., 2009). Accordingly, we find GFP distributed equally between cytoplasm and nucleus (predominantly nuclear in 4.9% of cells). Its localization shifts to the nucleus when fused to either a control NLS from the SV40 large T antigen (98.5% nuclear), JMY NLS-1 (95.6% nuclear), or JMY NLS-2 (83.2% nuclear; Figure 1, G and H). This demonstrates that both JMY NLS-1 and -2 are functional.

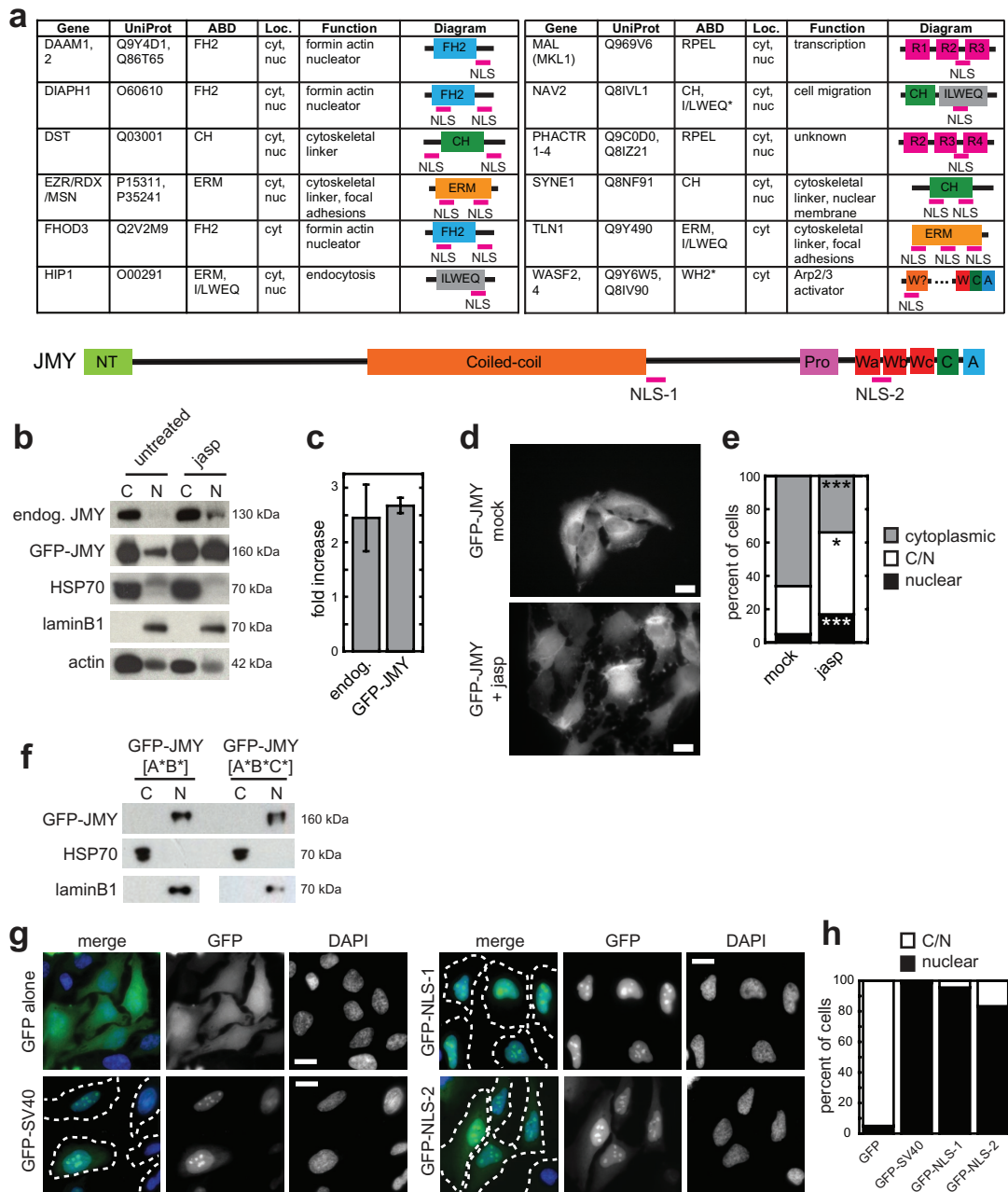


FIGURE 1: Actin regulates the subcellular localization of JMY. (A) Proteins with overlap between putative NLS and ABDs. The table indicates Uniprot number (<http://www.uniprot.org>), type of ABD, cellular localization (Loc.), function, and a diagram showing position of the putative NLS relative to the ABD. References and full gene names are found in Supplemental Table S1. Asterisk indicates putative (uncharacterized) ABD. Bottom, domain structure of JMY, showing position of putative NLSs (NLS-1, amino acids 603–620; NLS-2, 867–882). WH2s are abbreviated Wa, Wb, and Wc. Other domains illustrated are as follows: NT, N-terminal; Pro, polyproline; C, Central; A, acidic (Zuchero et al., 2009). (B, C) Endogenous and GFP-JMY accumulate in the nucleus following polymerization of actin with 500 nM jasp for 30 min. Following drug treatment, wild-type cells or cells stably expressing GFP-JMY were fractionated into cytoplasmic and nuclear pools (see Materials and Methods). Immunoblotting was performed to assess the localization of JMY, and fraction purity was determined by blotting with HSP70 (cytoplasmic marker) and lamin B1 (nuclear marker). (C) Quantification of immunoblots indicates that both endogenous and GFP-tagged JMY are ~2.5 times more nuclear in jasp-treated cells relative to untreated cells. Error bars, SEM; $n \geq 3$. (D, E) Analysis of GFP-JMY localization by microscopy. GFP-JMY accumulates in the nucleus in response to actin polymerization induced by jasplakinolide. JMY constructs were transiently expressed in HeLa cells for 16 h prior to treatment with jasp or DMSO (mock). (E) Quantification of ≥ 300 cells per condition, $n \geq 3$, showing percentage of cells that were predominantly cytoplasmic (gray), equally distributed in cytoplasm and nucleus (C/N, white) or predominantly nuclear (black). * $p < 0.05$, ** $p < 0.005$. (F) Actin-binding mutants GFP-JMY[A*B*] and GFP-JMY[A*B*C*] are completely nuclear. Cells were transfected and fractionated as in B. $n = 2$. (G, H) JMY NLS-1 and NLS-2 are functional NLS sequences. Tagging GFP with either a control NLS (SV40) or JMY NLS drives it into the nucleus. (G) Quantification of GFP localization in ≥ 130 cells per condition, $n = 2$. All scale bars, 20 μ m.

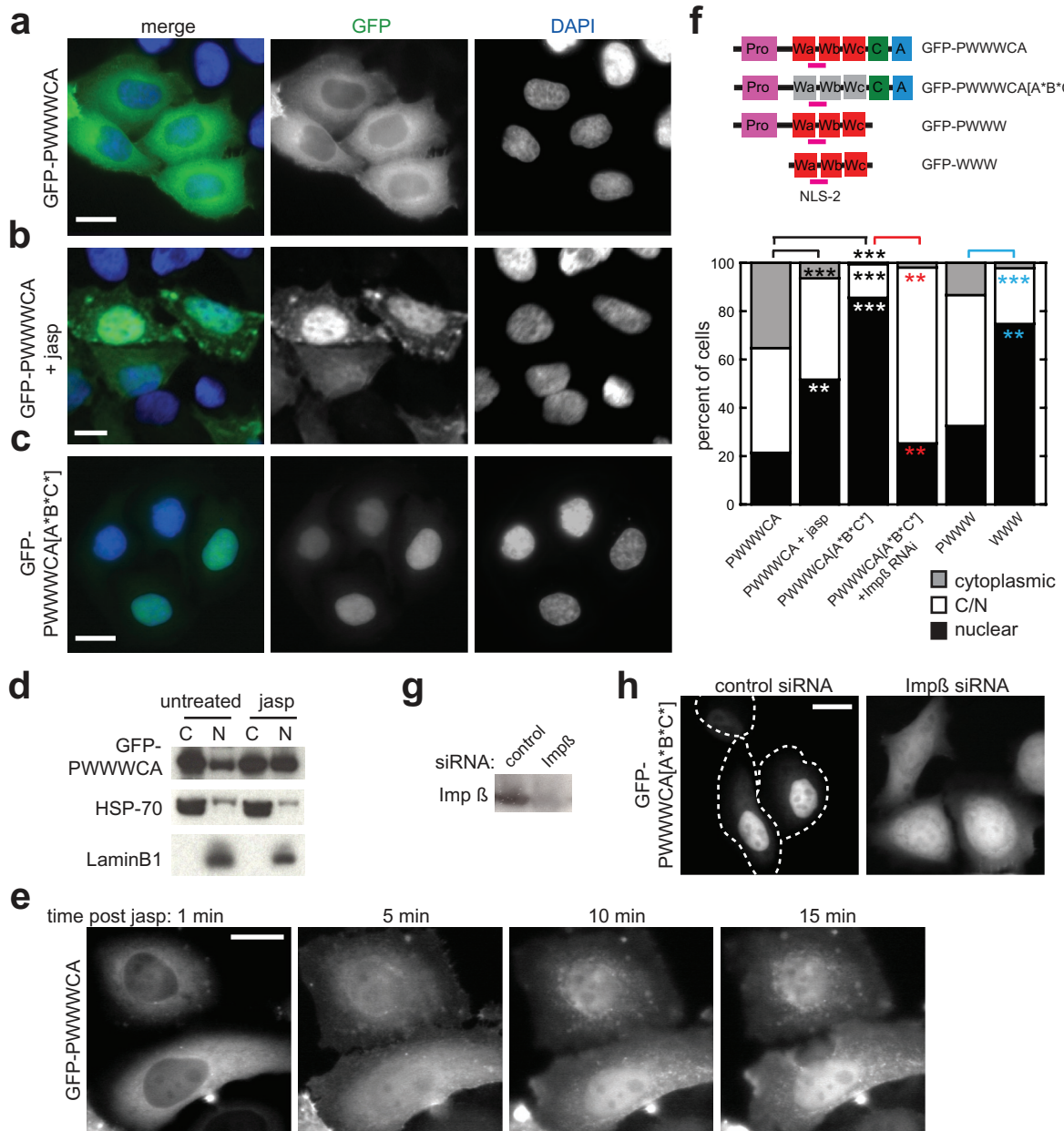


FIGURE 2: The C-terminus of JMY recapitulates actin-dependent localization. (A–C) Whereas GFP-PWWCAs is largely cytoplasmic (A), it accumulates in the nucleus following polymerization of actin with jasp (B) or when actin binding is blocked with WH2 point mutations (GFP-PWWCAs[A*B*C*]; C). Cells transiently transfected with GFP constructs were treated for 30 min with jasp as marked, then fixed and imaged. (D) Cellular fractionations as in Figure 1B show accumulation of GFP-PWWCAs in the nucleus following jasp treatment. (E) Time-lapse microscopy of GFP-PWWCAs following addition of 500 nM jasp. All scale bars, 20 μ m. (F) Top, diagram showing C-terminal JMY fragments. Bottom, quantification of microscopy in (a–h); >150 cells per condition, $n = 3$. ** $p < 0.01$; *** $p < 0.005$. Conditions are compared with GFP-PWWCAs alone, except where indicated with colored brackets. C/N, equally distributed in cytoplasm and nucleus. (G, H) Impβ is required for nuclear localization of the GFP-PWWCAs[A*B*C*] mutant. (G) Immunoblot showing that Impβ expression was knocked down by RNAi with an Impβ-specific siRNA but not control siRNA (see also Supplemental Figure S5, a). (H) RNAi of Impβ, but not control siRNA, causes GFP-PWWCAs[A*B*C*] localization to shift from exclusively nuclear to equally distributed between the nucleus and cytoplasm. This demonstrates that its normal nuclear localization is dependent on Impβ.

Actin-dependent localization of JMY is recapitulated by GFP-PWWCAs

We next asked whether the C-terminal (PWWCAs, where P stands for proline domain) region of JMY, which contains both the actin-binding WH2 domains and NLS-2, is sufficient for actin-dependent nuclear accumulation. Similar to full-length GFP-JMY, GFP-PWWCAs is largely cytoplasmic, or equally distributed between

the nucleus and cytoplasm, in most cells (only $21.4 \pm 3.0\%$ nuclear; Figure 2, A and F). It rapidly accumulates in the nucleus in response to actin polymerization by jasp, and its accumulation is more robust than that for full-length JMY ($6.5 \pm 0.2\%$ cytoplasmic, $51.8 \pm 5.1\%$ nuclear in jasp-treated cells; Figure 2, B and F). Cellular fractionation confirms this observation (Figure 2D), and time-lapse microscopy demonstrates that GFP-PWWCAs accumulates in the nucleus after

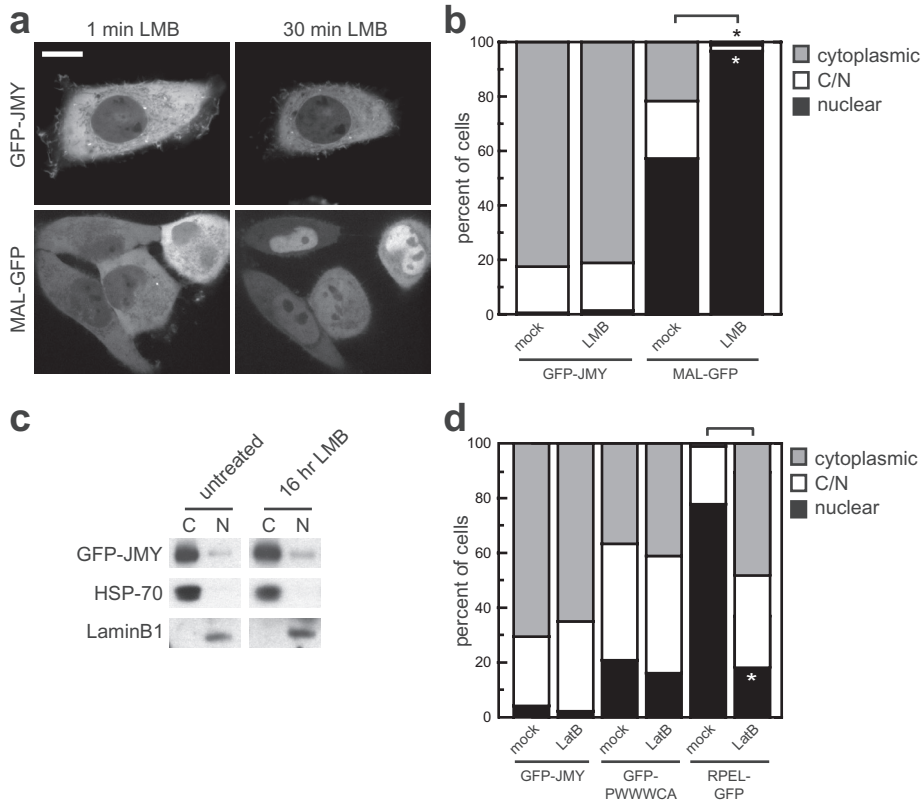


FIGURE 3: Nuclear accumulation of JMY is not regulated by export. (A–C). GFP-JMY does not accumulate in the nucleus following inhibition of Crm-1-dependent nuclear export by LMB. (A) Cells transiently transfected with GFP-JMY or MAL-GFP (control) were imaged immediately and 30 min after adding LMB. GFP-JMY remains in the cytoplasm, whereas MAL-GFP rapidly accumulates in the nucleus. Scale bars, 20 μ m. (B) Transiently transfected cells were treated with LMB as marked for 30 min, fixed, and imaged. LMB does not induce nuclear accumulation of JMY. In contrast, MAL-GFP is significantly more nuclear following LMB treatment. * $p < 0.05$. More than 100 cells per condition, $n = 2$. (C) Cellular fractionations show that JMY does not accumulate in the nucleus of cells grown overnight in the presence of LMB. (D) LatB drives export of RPEL-GFP but not of GFP-JMY or GFP-PWWWC. * $p < 0.05$; >100 cells per condition, $n = 3$ for all conditions, except GFP-PWWWC + Lat and RPEL-GFP + Lat, $n = 2$. C/N, equally distributed in cytoplasm and nucleus.

just 10–15 min of treatment (Figure 2E). WH2 point mutations that block actin binding (GFP-PWWWC[A*B*C*]) cause JMY localization to become almost entirely nuclear (85.1% nuclear; Figure 2, C and F). Of interest, although PWWW (lacking the CA domain) behaves similarly to PWWWC (32.4 \pm 3.0% nuclear), removing the polyproline domain (WWW) decreases the fraction of cells with nuclear JMY to 74.8 \pm 0.5% (Figure 2F and Supplemental Figure S3A; see Discussion).

Is the nuclear localization of GFP-PWWWC[A*B*C*] dependent on the classical nuclear import machinery of Imp α and Imp β ? Humans have several Imp α paralogues but only one Imp β (Quensel et al., 2004), so to test this we knocked down Imp β expression by RNAi (Figure 2G; see also Supplemental Figure S5A). In cells treated with Imp β small interfering RNA (siRNA), but not control siRNA, GFP-PWWWC[A*B*C*] loses its strict nuclear localization (Figure 2, F and H). This suggests that nuclear accumulation of JMY is due to regulated import and not diffusion through the nuclear pore.

Nuclear localization of JMY is not regulated by export

In addition to controlling the rate of nuclear import of JMY, does actin also control the rate of export? Our observation that actin polymerization causes JMY to accumulate in the nucleus can be ex-

plained by polymerization inducing either 1) an increase in the rate of nuclear import or 2) a decrease in the rate of nuclear export. For decreased export to promote nuclear accumulation, JMY would have to normally shuttle between the cytoplasm and nucleus. Arguing against the second model, we found that neither endogenous nor GFP-JMY accumulates in the nucleus after export is blocked with LMB for 30 min (GFP-JMY from 1.2 \pm 0.7% nuclear to 1.3 \pm 0.7% nuclear; Figure 3, A and B). Immunoblots of fractionated cells reveal no nuclear accumulation of GFP-JMY even when cells are grown overnight with LMB (Figure 3C). In contrast, MAL accumulates in the nucleus immediately after blocking of nuclear export with LMB (Vartiainen et al., 2007; Figure 3, A and B). This suggests that JMY does not normally shuttle between the cytoplasm and nucleus. JMY has no putative nuclear export signal (La Cour et al., 2004), but it remains possible that its export from the nucleus is independent of Crm-1 but dependent on actin. Depolymerizing actin with LatB induces cytoplasmic localization of MAL or the MAL RPEL cluster but has no significant effect on full-length GFP-JMY or GFP-PWWWC (Figure 3D). This is also true in DNA-damaged cells, in which basal GFP-JMY localization is more nuclear (Supplemental Figure S3B). Thus, export of JMY is not regulated by actin monomers.

Actin and importins compete for binding to JMY

The spatial overlap between the importin-binding NLS and actin-binding WH2 domains (Supplemental Figure S2C) suggests a model for how actin regulates JMY nuclear

import. Do actin monomers inhibit import of JMY by directly competing with the binding of importins? We developed a glutathione S-transferase (GST) pulldown assay that allows us to simultaneously detect binding of actin monomers, Imp α , and Imp β to GST-tagged JMY WWWCA or GST alone. Actin and importins bind to GST-JMY, whereas very little binds nonspecifically to GST alone (Figure 4, A and B). Titrating the actin monomer concentration shows that actin effectively competes Imp α/β off of GST-JMY (Figure 4, C and D). Competition is dose dependent and saturates at \sim 10 μ M, approximately the same concentration at which actin binding saturates. Using depletion of Imp α/β from the supernatant as an indirect readout of binding affinity, we confirmed that actin competes with binding of Imp α/β to JMY (Supplemental Figure S3G). Competition is greatly attenuated when the affinity for actin binding to WH2-a and WH2-b is weakened using the same mutations as in Figure 1 (see Supplemental Figure S3, C and D).

Imp α is normally autoinhibited but becomes able to bind an NLS following binding of Imp β (Fanara et al., 2000; Catimel et al., 2001). Accordingly, Imp α does not bind to GST-JMY in the absence of Imp β , demonstrating that the binding we see in the presence of the Imp α/β complex is specific (Figure 4, A and B). Imp β , however, binds directly to GST-JMY in the absence of Imp α . Although NLSs

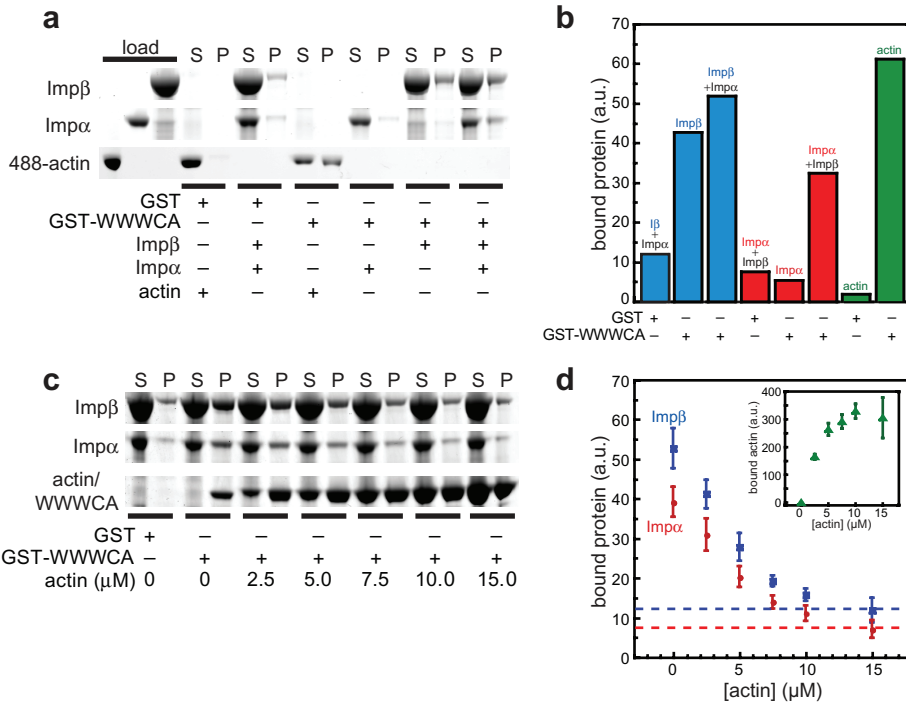


FIGURE 4: Importins and actin compete for binding to JMY. (A, B) GST pulldown showing that actin, Imp α , and Imp β bind to JMY GST-WWWCA. Following incubation of purified proteins with GST-WWWCA glutathione-Sepharose beads, the supernatant (S) was removed, the beads were washed, and bound proteins (P) were eluted. Actin (5% Alexa 488 labeled) was kept monomeric by the inclusion of 2x molar excess of LatB. Imp β binds even in the absence of Imp α , but Imp α binds only in the presence of Imp β , consistent with it being autoinhibited (Fanara et al., 2000). GST alone is used to show background, which is largely nonspecific binding to the resin. SDS-PAGE gels were first scanned for Alexa 488 actin and then stained with SYPRO Red to visualize proteins (see also full gel scan in Supplemental Figure S4, f). (B) Bound proteins were quantified using ImageQuant software. (C, D) Actin competes with Imp α / β for binding to JMY. GST-WWWCA beads were incubated with 2.5 μ M Imp α and Imp β and increasing concentrations of LatB-actin. By 10–15 μ M actin, actin binding has saturated and bound importin levels have been reduced to the level of nonspecific binding. (D) Quantification of bound Imp α and Imp β , showing the averages from three independent experiments. Inset, bound actin. Error bars, SEM.

are typically bound directly by Imp α , some arginine-rich NLSs (like JMY NLS-2) also interact directly with Imp β (Palmeri and Malim, 1999; Fontes et al., 2003).

Because actin and importins compete for binding to JMY and Imp β is sufficient to bind JMY, does Imp β block actin nucleation by JMY? We find that Imp β markedly decreases the rate of JMY-catalyzed actin polymerization in vitro but has no effect on actin polymerization in the absence of JMY or on Arp2/3 activation by a C-terminal fragment of JMY (WCA) lacking NLS-2 (Supplemental Figure S3, E and F, and data not shown). Nucleation activity is not completely blocked, and the decrease in activity saturates at approximately the same activity as a JMY fragment lacking WH2-a (JMY WWCA), suggesting that, at least in vitro, importins are only able to block actin from binding to WH2-a.

On the basis of these results, we tested whether this competition mechanism is conserved between JMY and MAL. MAL binds actin monomers using a cluster of three RPEL motifs (Miralles et al., 2003; Guettler et al., 2008) that overlap with a functional NLS (Vartiainen et al., 2007). Like JMY, MAL accumulates in the nucleus when actin polymerizes. We find that purified actin and importins also compete for binding to the MAL RPEL cluster (Supplemental Figure S5, A–E), consistent with recent findings (Pawlowski et al., 2010). Unlike JMY, MAL does not nucleate actin (Supplemental Figure S4F). These results

demonstrate that actin regulates JMY and MAL localization by the same mechanism: competing with importins for direct binding.

Importins and actin binding control DNA damage-induced nuclear accumulation of JMY

The established nuclear role of JMY is as a transcriptional coactivator of p53. DNA damage causes both increase in JMY expression and accumulation of JMY in the nucleus, where it potentiates p53-dependent transcription of proapoptotic genes (Shikama et al., 1999; Coutts et al., 2007). Does DNA damage trigger JMY localization to the nucleus by the same mechanism as the actin polymerization-induced accumulation that we have described? Recent work from several groups revealed that DNA damage induces polymerization of cytoplasmic actin (Levee et al., 1996; Guerra et al., 2008; Croft et al., 2011; Ishimoto et al., 2011). These studies were conducted using multiple cell types and genotoxic agents, suggesting that actin polymerization is a general response to DNA damage. On the basis of these results, we tested whether UV-induced DNA damage also promotes actin filament assembly. It is striking that we found that following DNA damage, actin polymer concentrations (measured by average cellular intensity of Alexa 568-phalloidin) nearly double (568-phalloidin intensity: untreated, 1.0 \pm 0.04 arbitrary fluorescence units; 12 h post-UV, 1.4 \pm 0.2; 24 h post-UV, 1.8 \pm 0.1; Figure 5, A and B). Of importance, the UV treatment conditions that induce actin polymerization are identical to those that cause JMY nuclear accumulation.

JMY accumulates in the nucleus following DNA damage caused by multiple agents, including UV irradiation, etoposide, and neocarzinostatin (Figure 5, C and D, and Supplemental Figure S5; see also Supplemental Figure S3B). Following UV treatment, GFP-JMY is predominantly nuclear in 54.6 \pm 3.2% of cells, compared with 4.1 \pm 1.4% of control cells. As expected, DNA damage-induced nuclear import of JMY requires Imp β (following UV treatment JMY is predominantly nuclear in only 2.6 \pm 1.6% of Imp β RNAi cells; Supplemental Figure S5, A–C). In contrast to full-length JMY, the truncation mutant Δ WWWCA does not accumulate in the nucleus in response to UV (percentage nuclear: pre-UV, 0.0 \pm 0%; post-UV, 0.4 \pm 0.4%; Figure 5, C and D) or etoposide (Supplemental Figure S5, D and E), demonstrating that this region, which contains NLS-2 (but not NLS-1), is required for DNA damage-induced nuclear import. The truncation mutant Δ CA, which lacks its Arp2/3-binding site but still contains NLS-2 and the WH2 domains, is indistinguishable from full-length JMY (Supplemental Figure S5D). Together, these results suggest that DNA damage causes JMY nuclear accumulation by driving actin polymerization, which reduces actin monomers bound to JMY and allows for importin-dependent nuclear import.

DISCUSSION

Previous work demonstrated that, in response to DNA damage, JMY accumulates in the nucleus and promotes p53-mediated

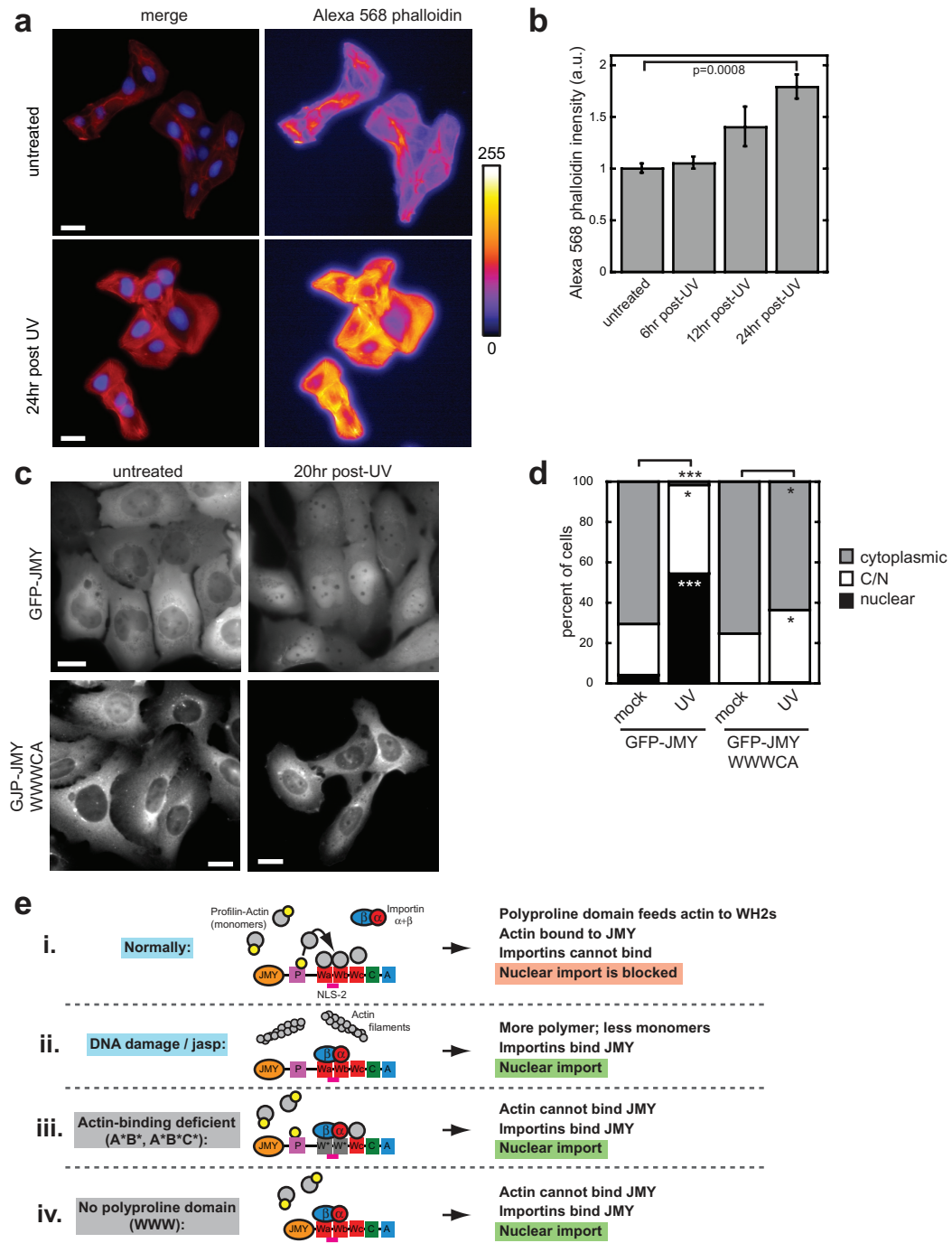


FIGURE 5: Importins and actin binding control DNA damage–induced nuclear accumulation of JMY. (A, B) Actin polymerizes in U2OS cells in response to DNA damage induced by UV irradiation (50 J/m^2). Cells were treated with UV at staggered start times and fixed at the same time and then stained with Alexa 568–phalloidin (see Materials and Methods). (A) Untreated cells (top) and cells 24 h after UV treatment (bottom). Left, merged images of Alexa 568–phalloidin and DAPI. Right, Alexa 568–phalloidin images are false colored to show intensity (ImageJ). Scale bars, 5 μm . (B) Quantification of average cellular Alexa 568–phalloidin intensity in cells without and at several time points after UV treatment. $n = 4$ coverslips, on two separate days. (C, D) GFP-JMY, but not Δ WWWCA (Zuchero et al., 2009) were imaged before and 20 h after UV treatment (50 J/m^2). Scale bars, 10 μm . (D) Quantification of >240 cells per condition, $n = 3$. C/N, equally distributed in cytoplasm and nucleus. * $p < 0.05$, ** $p < 0.005$. (E) Model of how actin regulates nuclear import of JMY. (i) In untreated cells, the polyproline domain feeds free actin monomers to JMY WH2 domains, which blocks binding of importins, keeping JMY in the cytoplasm. (ii) Following DNA damage or treatment with jasp, actin polymerizes. This decreases the concentration of free monomer and allows importins to bind JMY and import it into the nucleus. (iii) In the case of actin-binding mutants (e.g., GFP-JMY[A*B*]), importins can constitutively bind and import JMY into the nucleus. (iv) JMY lacking the polyproline domain may be unable to bind actin monomers, making this mutant equivalent to actin binding–deficient mutants.

apoptosis. We find that this DNA damage–induced nuclear accumulation requires a nuclear localization sequence in JMY buried within a cluster of actin monomer-binding sites. We also find that monomeric actin regulates JMY’s nuclear import by blocking interaction with the import machinery. These results argue that nuclear accumulation of JMY may be triggered by DNA damage–induced actin assembly. Consistent with this idea, we observed that DNA damage induces robust actin polymerization, nearly doubling the filamentous actin concentration in the cytoplasm and significantly reducing the concentration of monomeric actin. This observation fits with previous studies demonstrating DNA damage–induced actin assembly (Levee et al., 1996) and identifying a Rho-dependent pathway that links DNA damage to actin filament assembly (Croft et al., 2005, 2011).

Is it possible that JMY’s localization is dependent on binding to filamentous actin? We showed previously that, *in vitro*, JMY binds monomeric actin but does not appreciably copellet with filamentous actin or cap filament ends (Zuchero et al., 2009). In cells JMY does not localize strongly to actin-rich structures such as stress fibers, nor does depolymerizing actin filaments with LatB affect JMY localization. Together these results argue that actin filaments do not directly influence JMY’s subcellular localization.

The localization of both JMY and the MRTF family member MAL is determined by competition between actin monomers and the nuclear import machinery, but regulation of the two proteins is not identical. For example, when MAL is concentrated in the nucleus, treatment of cells with latrunculin B causes it to move into the cytoplasm (Vartiainen et al., 2007; Figure 3D), consistent with the fact that MAL shuttles continuously between the two compartments and can be trapped in the cytoplasm by association with newly liberated actin monomers. In contrast, latrunculin does not deplete JMY from nuclei of cells with damaged DNA (Supplemental Figure S3B), consistent with our observation that JMY does not cycle between nucleus and cytoplasm (Figure 3, A–C). Why does MAL cycle between nucleus and cytoplasm, whereas JMY does not? The difference could reflect tighter inhibition of nuclear import by the WH2–actin complexes of JMY than that of the RPEL–actin complexes of MAL, or it could reflect stable association of JMY with nuclear partners, perhaps components of the DNA damage response (Shikama et al., 1999; Demonacos et al., 2001).

The lack of continuous cycling means that once JMY is in the nucleus its localization is insensitive to changes in cytoplasm actin. In this way JMY’s nuclear localization performs like a toggle switch: a transient dip in monomeric actin concentration produces prolonged nuclear accumulation. This is probably important for its cellular function. For example, JMY promotes initiation of apoptosis and, early in this process, the concentration gradient of Ran-GTP between the nucleoplasm and cytoplasm collapses, trapping many NLS-containing proteins in the cytoplasm bound to Imp α/β (Wong et al., 2009). If JMY shuttled back and forth, it would not remain in the nucleus of apoptotic cells. In later stages of apoptosis the concentration of monomeric actin increases (Suarez-Huerta et al., 2000), which would also trap rapidly shuttling JMY molecules in the cytoplasm.

Once in the nucleus, does actin also contribute to JMY-mediated transcription? Coutts et al. (2009) found that JMY targeted to the nucleus with an NLS stimulates p53-dependent transcription of a reporter gene, and LatB blocks this. This suggests that the role of JMY in transcription either requires actin polymerization or is inhibited by actin monomers. Now that actin- and Arp2/3–binding mutants of JMY have been characterized, it will be interesting to test whether JMY promotes actin polymerization in the nucleus and whether it requires this for its role in activating p53. We show here that different actin-binding mutations can perturb the localization of

JMY, so it will be essential to take this into consideration when comparing the phenotypes of mutants.

How is JMY’s actin assembly activity regulated in cells? Recent cell biological experiments suggest that, *in vivo*, JMY activity is regulated by interaction with inhibitory binding partners. One obvious potential regulator is the nuclear import machinery, specifically the importin α/β complex (Supplemental Figure S4, D and E). The inhibitory effect of Imp β , however, relies on direct competition with monomeric actin, which has a cytoplasmic concentration at least 20-fold higher than that of Imp β (Gordon et al., 1976; Görlich et al., 1994). It is therefore extremely unlikely that importins regulate JMY activity *in vivo*.

Of interest, JMY requires its polyproline domain for retention in the cytoplasm (Figure 2F and Supplemental Figure S3A). Most proteins that activate the Arp2/3 complex contain a polyproline domain N-terminal to the WCA region (Rottner et al., 2010), and it is believed that polyproline domains facilitate the recruitment of profilin-bound actin monomers to Arp2/3 activators (Witke, 2004). Because the polymerizable pool of actin monomers in cells is largely bound to profilin (Kaiser et al., 1999), without the polyproline sequence it is possible that occupancy of the WH2 domains by actin is low, making this mutant equivalent to PWWWCA[A*B*C*]. Thus JMY could potentially be regulated by a protein that binds directly to its polyproline domain.

In addition to JMY and MAL, we identified 26 other actin-binding proteins with putative NLSs. It will be interesting to test whether any of these plays a role in actin assembly in the nucleus. Of particular interest are the 14 with overlap between ABD and NLS. Although most do not appear to shuttle in an actin-dependent manner, it is possible that their actin-regulatory activities are regulated by importin binding (and RanGTP). This could allow for control of their activities in the interphase nucleus or around mitotic chromosomes, similar to spindle factors, including the microtubule-organizing proteins TPX2 (Gruss et al., 2001) and NuMA (Nachury et al., 2001; Wiese et al., 2001), and nuclear lamins (Tsai et al., 2006). Future work will test the role of these proteins in coupling actin dynamics with nuclear and mitotic events.

MATERIALS AND METHODS

Bioinformatics

Canonical domain alignments of well-characterized ABDs, including monomer-binding families (WH2, RPEL) and filament-binding families (calponin homology, formin homology 2, ILWEQ, ezrin/radixin/moesin), were generated from published alignments supplemented with results of a high-stringency National Center for Biotechnology Information (NCBI) protein Basic Local Alignment Search Tool (pBLAST) search (*e* value, <0.00001) to ensure alignment diversity. Human proteins containing putative ABDs were identified using a low-stringency NCBI BLASTp search (*e* value, <0.05) based on similarity to members of canonical domain alignments. ABD- and NLS-containing candidates were identified from these results based on the presence of 1) one or more sequence motifs identified by NLS regular expression patterns from the NLSdb (<http://rostlab.org/services/nlsdb/>), 2) detectable conservation within the characterized actin-binding sites within each ABD using BLASTp (*e* value, <0.00001 for actin-binding sites >50 residues in length; any detectable similarity for actin-binding sites <50 residues), and 3) <5 residues of separation between putative NLS and ABD regions.

Molecular biology

Constructs were cloned from full-length mouse JMY or MAL using standard techniques. Primer sequences are available upon request.

JMY mutations are as follows: A*B*C* refers to triplicate mutations in each WH2 to block actin binding, in WH2-a (LF857AA, L870A), WH2-b (VL889AA, L900A), and WH2-c (IL920AA, L930A). Amino acid numbers of JMY constructs are as follows: GFP-PWWWCA, 791–983; GFP-PWWW, 791–938; GFP-WWW, 853–938; GFP-JMY Δ CA, 1–938; GFP-JMY Δ WWWCA, 1–852. MAL constructs are as follows: full-length MAL-GFP, 1–1021; RPEL-GFP, 2–261. The numbering of mouse MAL begins at leucine –92 (Miralles et al., 2003). All constructs were sequenced to ensure no mutations were introduced during cloning. We used pEGFP-C1 and pEGFP-N3 (Clontech, Mountain View, CA) as host vectors for making enhanced GFP fusions.

Cell culture

HeLa and U2OS cells (American Type Culture Collection, Manassas, VA) were cultured in DMEM supplemented with 10% fetal bovine serum, 2 mM L-glutamine, nonessential amino acids, and penicillin-streptomycin (University of California, San Francisco, Cell Culture Facility, San Francisco, CA) at 37°C with 5% CO₂. For transfection, cells were seeded onto glass coverslips overnight and transfected with GFP constructs using Lipofectamine LTX (Invitrogen, Carlsbad, CA), according to the manufacturer's protocol. For Imp β 1 RNAi, GFP-JMY stable cells (Zuchero et al., 2009) were transfected with 100 nM nontargeting (Stealth Medium GC#2; Invitrogen) or Imp β 1 siRNA (targeting bases 497–521 of human Imp β mRNA; Miki et al., 2008; purchased from Invitrogen), using Lipofectamine 2000 according to manufacturer's protocols, and grown for 3 d prior to UV treatment. Alternatively, siRNA and plasmid DNA were cotransfected using Lipofectamine 2000. For immunofluorescence, cells were fixed for 30 min in 3.2% formaldehyde in phosphate-buffered saline (PBS). Cells were then permeabilized with 0.1% Triton-X-100 in PBS, and nuclei were stained with 0.5 µg/ml 4',6-diamidino-2-phenylindole (DAPI; Sigma-Aldrich, St. Louis, MO). Fixed samples were mounted with fluorescent mounting medium (DakoCytomation, Hamburg, Germany).

Microscopy

Epifluorescence and wide-field images were acquired on a TE300 inverted microscope (Nikon, Melville, NY) equipped with a Hamamatsu C4742-98 cooled charge-coupled device camera (Hamamatsu, Hamamatsu, Japan), using 100x and 60x, 1.4 numerical aperture, Plan Apo objectives (Nikon) with MicroManager software (Stuurman et al., 2007). We used ImageJ (National Institutes of Health, Bethesda, MD) and Adobe Photoshop (Adobe, San Jose, CA) for image analysis and contrast adjustment. For live-cell imaging, cells were transfected, split onto glass coverslips after 18–24 h, and then given fresh medium with drugs or vehicle and kept at 37°C during image acquisition. Stable lines of U2OS cells expressing GFP-JMY were described previously (Zuchero et al., 2009). Localization of GFP fusion proteins was scored as predominantly cytoplasmic, equally distributed between the cytoplasm and nucleus (C/N), or predominantly cytoplasmic by an observer blind to the experimental condition (Guettler et al., 2008). Percentages presented in the text refer to percentage of cells in each category, unless otherwise indicated.

Drug treatments and UV irradiation

Jasplakinolide (Calbiochem, La Jolla, CA) and latrunculin B (Biomol International, Enzo Life Sciences, Plymouth, PA) were used at 500 nM in medium, and treatments were for 30 min. Leptomycin B (Sigma-Aldrich) was used at 20 nM for 30 min or 16 h, as noted. Etoposide (Sigma-Aldrich) was used at 10 µM, and neocarzinostatin

(Sigma-Aldrich) was used at 200 ng/ml. We made working stocks of all drugs or vehicle (dimethyl sulfoxide for LatB and jasp; methanol for LMB) in warm medium, replaced old medium with drugged medium, and incubated for the given time at 37° with 5% CO₂. Following treatment, cells were washed twice with warm PBS prior to fractionation or fixation for microscopy. For UV irradiation, medium was fully aspirated from cells, and they were subjected to a dose of 50 J/m² short-wave UV (0.5 mW/cm² for 10 s) in a GS Genelinker UV chamber (Bio-Rad, Hercules, CA; to achieve this low fluence rate, we needed to remove bulbs from the UV chamber). Fresh, warm medium was immediately added, and cells were returned to the incubator for the indicated time before fixing for imaging.

For calculation of phalloidin intensities, U2OS cells were UV treated at staggered times, so that all conditions were fixed at the same time postplating. Cells were fixed and permeabilized as described, stained for 15 min with 0.7 U/ml Alexa Fluor 568-phalloidin (Invitrogen), washed three times, and mounted as described. Four coverslips per condition, on two separate experimental days, were imaged. Ten micrographs per coverslip (>500 cells per coverslip, spanning the entire coverslip) were acquired blindly by focusing on the DAPI channel. Average cellular phalloidin intensity was measured in regions of interest containing all cells, using ImageJ. Slide background intensity was subtracted, and values were normalized by dividing by the average intensity of untreated cells.

Cellular fractionations

Approximately 1 × 10⁶ cells were harvested, washed with ice-cold PBS, and resuspended in hypotonic buffer (10 mM 4-(2-hydroxyethyl)-1-piperazineethanesulfonic acid [HEPES], pH 7.5, 10 mM KCl, 1.5 mM MgCl₂, 0.5 mM dithiothreitol, 5 µg/ml aprotinin, 15 µg/ml benzamidine, 10 µg/ml leupeptin, 5 µg/ml pepstatin A, 1 mM phenylmethanesulfonyl fluoride, and 40 µg/ml soybean trypsin inhibitor). Cells were pelleted in a microfuge by spinning at 1000 rpm for 5 min at 4°C and then lysed on ice for 10 min in hypotonic buffer plus 0.5% NP-40. Nuclei were pelleted by spinning at 3000 rpm for 2 min as described, and cytoplasmic fraction was aspirated and held on ice. Nuclei were washed with hypotonic buffer, assessed for quality by phase contrast microscopy, transferred to a new tube, and lysed in 8 M urea plus sample buffer, then boiled and sonicated prior to SDS-PAGE. For each fractionation experiment we blotted against HSP70 (cytoplasmic marker) and lamin B1 (nuclear marker) to monitor separation of cytoplasmic and nuclear fractions. Standard methods were used for immunoblotting, using 1:500 dilutions of 1289 (Coutts et al., 2007) and YA16 (Santa Cruz Biotechnology, Santa Cruz, CA) anti-JMY primary antibodies, mouse anti-lamin B1 (Invitrogen), mouse anti-HSP70 (Santa Cruz Biotechnology), 1:200 goat anti-Imp β (Santa Cruz Biotechnology), or 1:1000 mouse anti-actin JLA20 (Calbiochem). Horseradish peroxidase-conjugated secondaries (Jackson ImmunoResearch Laboratories, West Grove, PA) were used at 1:10,000, and ECL reagent (SuperSignal West Pico, Pierce, Rockford, IL) was used according to the manufacturer's instructions.

For quantification, subsaturated immunoblots were scanned (bands were deemed subsaturated if they were still translucent, i.e., text could be read through the band), and band intensity was measured and background subtracted in ImageJ. We measured relative nuclear JMY signal between jasp-treated and untreated cell lysates in the same blot. Measuring this ratio in several exposures of the same immunoblot confirmed that this ratio did not vary appreciably with different blot exposure intensities, provided they were subsaturated. Thus we could compare several experimental replicates without having to precisely match exposure intensity.

Biochemistry

JMY and MAL fragments were expressed as GST fusions in *Escherichia coli* and purified using a combination of glutathione and cation chromatography. For actin polymerization experiments the GST was removed to prevent dimerization of the recombinant protein. We used JMY(C978S) for biochemistry to improve reproducibility (Zuchero et al., 2009). Recombinant NusA-hexahistidine-tagged Imp β was purified by cobalt chromatography, removal of the NusA tag by cleavage with trypsin, and gel filtration on a Superdex 200 column. Protein concentrations were calculated using predicted molar extinction coefficients for JMY peptides (ProtParam, <http://web.expasy.org/protparam/>) or by quantitative SDS-PAGE with SYPRO Red staining (Invitrogen).

For GST pulldowns, 10 μ M GST-tagged proteins or GST alone was bound to glutathione-Sepharose 4B (GE Healthcare, Piscataway, NJ) or glutathione magnetic beads (Pierce) in PBS, 0.5 μ M TCEP, and 20% glycerol, with rotation, for 2–16 h at 4°, then washed three times to remove unbound protein. Note that background binding of proteins to glutathione magnetic beads (GST-MAL experiments) is much reduced compared with glutathione-Sepharose beads (GST-JMY experiments). Loaded beads (GST fusion proteins at ~1 μ M in final reaction volume) were rotated with proteins or protein storage buffer in PBS, 0.5 μ M tris(2-carboxyethyl)phosphine (TCEP), and 5 mg/mL bovine serum albumin (carrier) for 2–3 h at 4°C. As noted, 2.5 μ M each Imp α and Imp β was used. Actin was kept monomeric by using 2x molar equivalent of LatB. Beads were pelleted by centrifugation or magnetic separation, supernatant removed, and washed three times with PBS + 0.01% NP-40, transferring to a new tube in the final wash to prevent eluting protein non-specifically adsorbed to the tube wall. Bound proteins were recovered in sample buffer (same volume as reactions), and samples were analyzed by SDS-PAGE (NuPage gradient gels; GE Healthcare) with SYPRO Red staining and quantified by using a multiformat imager (Typhoon 9400; GE Healthcare) and ImageQuant software (GE Healthcare). SYPRO Red binds to SDS, and thus the measured fluorescence reflects mass of protein; we divided values by the molecular weight of the protein (42,000 Da for actin, 97,000 Da for Imp β , and 60,000 Da for Imp α) to calculate bound protein in relative molar terms. For visualization of Alexa 488-labeled actin, gels were scanned (Typhoon 9400) prior to SYPRO Red staining.

Actin polymerization assays

Actin was purified from *Acanthamoeba castellanii* as described (Gordon et al., 1976), labeled with pyrene iodoacetamide or Alexa 488 C5 maleimide as described (Cooper et al., 1983; Akin and Mullins, 2008), stored in buffer A (0.2 mM ATP, 0.5 mM TCEP, 0.1 mM CaCl₂, 0.02% wt/vol sodium azide, 2 mM Tris, pH 8.0, at 4°C), and gel filtered before use. *Acanthamoeba* actin is 95.5% identical, 99.2% conserved with regard to human β -actin (compared with human or rabbit skeletal muscle actin, 92.8% identical), and so represents a better model of cytoplasmic actin than skeletal muscle actin. Arp2/3 was purified from *Acanthamoeba* as described (Dayel et al., 2001) and flash frozen with 10% glycerol. Actin polymerization assays were performed as described (Zuchero et al., 2009) in 1x KMEH (50 mM KCl, 1 mM MgCl₂, 1 mM ethylene glycol tetraacetic acid [EGTA], 10 mM HEPES, pH 7.0). Ca²⁺-actin was converted into Mg²⁺-actin by incubation of actin in ME (50 mM MgCl₂, 0.2 mM EGTA) for 2 min prior to adding 10x KMEH and test components. Pyrene fluorescence was measured with a Synergy 4 plate reader and Gen5 software (BioTek, Winooski, VT). Unless otherwise noted, polymerization reactions contained 4 μ M actin (5% pyrene labeled) and 250 nM JMY. Importin competition reactions contained 200 nM

CT-JMY (amino acids 583–983, encompassing both NLS sequences) and 5 μ M Imp β or an equivalent volume of Imp β storage buffer. For half-time calculations, reactions were normalized by zeroing traces, dividing by the plateau value, and solving for time at half-maximal fluorescence (0.5 a.u.). All error values are SEM. We used two-tailed unpaired t tests, assuming unequal variance, to calculate p values (Excel; Microsoft, Redmond, WA).

ACKNOWLEDGMENTS

This work began in the 2008 Physiology Course at the Marine Biological Laboratory in Woods Hole with the talents and creativity of D. Shane Courson, P. Myron Miller, and H. Hewitt Tuson. We are greatly indebted to Yoshihiro Yoneda, Takashi Miki, and Peter Bieling for advice and generously providing importin constructs and proteins. This work was supported by grants from the National Institutes of Health, an American Heart Association Predoctoral Fellowship (J.B.Z.), the Robert Day Allen Fellowship Fund (J.B.Z.), and a National Science Foundation Predoctoral Fellowship (B.B.). We thank members of the Mullins and Vale labs, especially Orkun Akin, Scott Hansen, and Ron Vale, as well as Margot Quinlan and the Cell Division Group at the Marine Biological Laboratory, for reagents, helpful discussions, and critical reading of the manuscript.

REFERENCES

- Akin O, Mullins RD (2008). Capping protein increases the rate of actin-based motility by promoting filament nucleation by the Arp2/3 complex. *Cell* 133, 841–851.
- Bubb MR, Senderowicz AM, Sausville EA, Duncan KL, Korn ED (1994). Jasplakinolide, a cytotoxic natural product, induces actin polymerization and competitively inhibits the binding of phalloidin to F-actin. *J Biol Chem* 269, 14869–14871.
- Bubb MR, Spector I, Beyer BB, Fosen KM (2000). Effects of jasplakinolide on the kinetics of actin polymerization. An explanation for certain *in vivo* observations. *J Biol Chem* 275, 5163–5170.
- Catimel B, Teh T, Fontes MR, Jennings IG, Jans DA, Howlett GJ, Nice EC, Kobe B (2001). Biophysical characterization of interactions involving importin-alpha during nuclear import. *J Biol Chem* 276, 34189–34198.
- Cooper JA, Walker SB, Pollard TD (1983). Pyrene actin: documentation of the validity of a sensitive assay for actin polymerization. *J Muscle Res Cell Motil* 4, 253–262.
- Coutts AS, Boulahbel H, Graham A, La Thangue NB (2007). Mdm2 targets the p53 transcription cofactor JMY for degradation. *EMBO Rep* 8, 84–90.
- Coutts A, Weston L, La Thangue NB (2009). A transcription co-factor integrates cell adhesion and motility with the p53 response. *Proc Natl Acad Sci USA* 106, 19872–19877.
- Croft DR, Coleman ML, Li S, Robertson D, Sullivan T, Stewart CL, Olson MF (2005). Actin-myosin-based contraction is responsible for apoptotic nuclear disintegration. *J Cell Biol* 168, 245–255.
- Croft DR et al. (2011). p53-mediated transcriptional regulation and activation of the actin cytoskeleton regulatory RhoC to LIMK2 signaling pathway promotes cell survival. *Cell Res* 21, 666–682.
- Dayel MJ, Holleran EA, Mullins RD (2001). Arp2/3 complex requires hydrolyzable ATP for nucleation of new actin filaments. *Proc Natl Acad Sci USA* 98, 14871–14876.
- Demonacos C, Krstic-Demonacos M, La Thangue NB (2001). A TPR motif cofactor contributes to p300 activity in the p53 response. *Mol Cell* 8, 71–84.
- Fanara P, Hodel MR, Corbett AH, Hodel AE (2000). Quantitative analysis of nuclear localization signal (NLS)-importin alpha interaction through fluorescence depolarization. Evidence for auto-inhibitory regulation of NLS binding. *J Biol Chem* 275, 21218–21223.
- Firat-Karalar EN, Hsieh PP, Welch MD (2011). The actin nucleation factor JMY is a negative regulator of neuritogenesis. *Mol Biol Cell* 22, 4563–4574.
- Fontes MR, Teh T, Jans D, Brinkworth RI, Kobe B (2003). Structural basis for the specificity of bipartite nuclear localization sequence binding by importin-alpha. *J Biol Chem* 278, 27981–27987.

- Gordon DJ, Eisenberg E, Korn ED (1976). Characterization of cytoplasmic actin isolated from *Acanthamoeba castellanii* by a new method. *J Biol Chem* 251, 4778–4786.
- Görlich D, Prehn S, Laskey LA, Hartmann E (1994). Isolation of a protein that is essential for the first step of nuclear protein import. *Cell* 79, 767–778.
- Gruss OJ, Carazo-Salas RE, Schatz CA, Guarguaglini G, Kast J, Wilm M, Le Bot N, Vernos I, Karsenti E, Mattaj JW (2001). Ran induces spindle assembly by reversing the inhibitory effect of importin alpha on TPX2 activity. *Cell* 104, 83–93.
- Guerra L, Carr HS, Richter-Dahlfors A, Masucci MG, Thelestam M, Frost JA, Frisan T (2008). A bacterial cytotoxin identifies the RhoA exchange factor Net1 as a key effector in the response to DNA damage. *PLoS One* 3, e2254.
- Guettler S, Vartiainen MK, Miralles F, Larjani B, Treisman R (2008). RPEL motifs link the serum response factor cofactor MAL but not myocardin to Rho signaling via actin binding. *Mol Cell Biol* 28, 732–742.
- Ishimoto T, Ozawa T, Mori H (2011). Real-time monitoring of actin polymerization in living cells using split luciferase. *Bioconjug Chem* 22, 1136–1144.
- Kaiser DA, Vinson VK, Murphy DB, Pollard TD (1999). Profilin is predominantly associated with monomeric actin in *Acanthamoeba*. *J Cell Sci* 112, 3779–3790.
- Kelly A, Kranitz H, Dötsch V, Mullins R (2006). Actin binding to the central domain of WASP/Scar proteins plays a critical role in the activation of the Arp2/3 complex. *J Biol Chem* 281, 10589–10597.
- Kiuchi T, Nagai T, Ohashi K, Mizuno K (2011). Measurements of spatiotemporal changes in G-actin concentration reveal its effect on stimulus-induced actin assembly and lamellipodium extension. *J Cell Biol* 193, 365–380.
- la Cour T, Kiemer L, Mølgaard A, Gupta R, Skriver K, Brunak S (2004). Analysis and prediction of leucine-rich nuclear export signals. *Protein Eng Des Sel* 17, 527–536.
- Levee MG, Dabrowska MI, Lelli JL Jr, Hinshaw DB (1996). Actin polymerization and depolymerization during apoptosis in HL-60 cells. *Am J Physiol* 271, C1981–C1992.
- Lyubimova A, Bershadsky AD, Ben-Ze'ev A (1997). Autoregulation of actin synthesis responds to monomeric actin levels. *J Cell Biochem* 65, 469–478.
- Miki T, Okawa K, Sekimoto T, Yoneda Y, Watanabe S, Ishizaki T, Narumiya S (2008). mDia2 shuttles between the nucleus and the cytoplasm through the importin-alpha/beta- and CRM1-mediated nuclear transport mechanism. *J Biol Chem* 284, 5753–5762.
- Miralles F, Posern G, Zaromytidou AI, Treisman R (2003). Actin dynamics control SRF activity by regulation of its coactivator MAL. *Cell* 113, 329–342.
- Mohr D, Frey S, Fischer T, Gütter T, Görlich D (2009). Characterisation of the passive permeability barrier of nuclear pore complexes. *EMBO J* 28, 2541–2553.
- Nachury MV, Maresca TJ, Salmon WC, Waterman-Storer CM, Heald R, Weis K (2001). Importin beta is a mitotic target of the small GTPase Ran in spindle assembly. *Cell* 104, 95–106.
- Nair R, Carter P, Rost B (2003). NLSdb: database of nuclear localization signals. *Nucleic Acids Res* 31, 397–399.
- Palmeri D, Malim MH (1999). Importin beta can mediate the nuclear import of an arginine-rich nuclear localization signal in the absence of importin alpha. *Mol Cell Biol* 19, 1218–1225.
- Pawlowski R, Rajakylä EK, Vartiainen MK, Treisman R (2010). An actin-regulated importin alpha/beta-dependent extended bipartite NLS directs nuclear import of MRTF-A. *EMBO J* 29, 3448–3458.
- Quensel C, Friedrich B, Sommer T, Hartmann E, Kohlerl M (2004). In vivo analysis of importin alpha proteins reveals cellular proliferation inhibition and substrate specificity. *Mol Cell Biol* 24, 10246–10255.
- Quinlan ME, Heuser JE, Kerkhoff E, Mullins RD (2005). *Drosophila* Spire is an actin nucleation factor. *Nature* 433, 382–388.
- Rottner K, Hänsch J, Campellone KG (2010). WASH, WHAMM and JMY: regulation of Arp2/3 complex and beyond. *Trends Cell Biol* 20, 650–661.
- Sagara J, Arata T, Taniguchi S (2009). Scapin, the protein phosphatase 1 binding protein, enhances cell spreading and motility by interacting with the actin cytoskeleton. *PLoS One* 4, e4247.
- Shikama N, Lee CW, France S, Delavaine L, Lyon J, Krstic-Demonacos M, La Thangue NB (1999). A novel cofactor for p300 that regulates the p53 response. *Mol Cell* 4, 365–376.
- Spector I, Shochet NR, Kashman Y, Graweiss A (1983). Latrunculins: novel marine toxins that disrupt microfilament organization in cultured cells. *Science* 219, 493–495.
- Strasser GA, Rahim NA, VanderWaal KE, Gertler FB, Lanier LM (2004). Arp2/3 is a negative regulator of growth cone translocation. *Neuron* 43, 81–94.
- Stuurman N, Amodaj N, Vale RD (2007). Micro-Manager: open source software for light microscope imaging. *Microsc Today* 15, 42–43.
- Suarez-Huerta N, Mosselmans R, Dumont JE, Robaye B (2000). Actin depolymerization and polymerization are required during apoptosis in endothelial cells. *J Cell Physiol* 184, 239–245.
- Tsai M-Y, Wang S, Heidinger JM, Shumaker DK, Adam SA, Goldman RD, Zheng Y (2006). A mitotic lamin B matrix induced by RanGTP required for spindle assembly. *Science* 311, 1887–1893.
- Vartiainen MK, Guettler S, Larjani B, Treisman R (2007). Nuclear actin regulates dynamic subcellular localization and activity of the SRF cofactor MAL. *Science* 316, 1749–1752.
- Welch MD, Mullins RD (2002). Cellular control of actin nucleation. *Annu Rev Cell Dev Biol* 18, 247–288.
- Wiese C, Wilde A, Moore MS, Adam SA, Merdes A, Zheng Y (2001). Role of importin-beta in coupling Ran to downstream targets in microtubule assembly. *Science* 291, 653–656.
- Witke W (2004). The role of profilin complexes in cell motility and other cellular processes. *Trends Cell Biol* 14, 461–469.
- Wolff B, Sanglier JJ, Wang Y (1997). Leptomycin B is an inhibitor of nuclear export: inhibition of nucleo-cytoplasmic translocation of the human immunodeficiency virus type 1 (HIV-1) Rev protein and Rev-dependent mRNA. *Chem Biol* 4, 139–147.
- Wong CH, Chan H, Ho CY, Lai SK, Chan KS, Koh CG, Li HY (2009). Apoptotic histone modification inhibits nuclear transport by regulating RCC1. *Nat Cell Biol* 11, 36–45.
- Zuchero JB, Coutts AS, Quinlan ME, La Thangue NB, Mullins RD (2009). p53-cofactor JMY is a multifunctional actin nucleation factor. *Nat Cell Biol* 11, 451–459.

Supplemental Information for:

**Actin Binding to WH2 Domains Regulates Nuclear Import of the
Multifunctional Actin Regulator JMY**

J. Bradley Zuchero, Brittany Belin & R. Dyche Mullins

Supplemental Methods

Bioinformatics

Sources of sequence alignments for ABD families are as follows: CH1, CH2, and CH3 (Bañuelos et al., 1998); ERM (Chishti et al., 1998; Sigrist et al., 2002); FH2 (Frazier and Field, 1997; Higgs, 2005; Schultz et al., 2000); I/LWEQ (McCann and Craig, 1997; Sigrist et al., 2002); RPEL (Mouilleron et al., 2008; Sigrist et al., 2002); and WH2 (Garner, Zuchero, and Mullins, unpublished). We found 120 proteins with significant alignment to an ABD (evalue <0.05). Confidence in a hit was decided based on whether this alignment contained known actin binding sequences (as opposed to just having homology to a region of the domain for which actin-binding has not been established) for CH1, CH2, and CH3 (Moores et al., 2000; Winder et al., 1995); ERM (Saleh et al., 2009); FH2 (Lu et al., 2007; Shimada et al., 2004); I/LWEQ (McCann and Craig, 1997); RPEL (Mouilleron et al., 2008); and WH2 (Chereau et al., 2005; Kelly et al., 2006; Panchal et al., 2003) domains.

Supplemental References

- Ahuja, R., R. Pinyol, N. Reichenbach, L. Custer, J. Klingensmith, M. Kessels, and B. Qualmann. 2007. Cordon-Bleu Is an Actin Nucleation Factor and Controls Neuronal Morphology. *Cell.* 131:337-350.
- Allen, P.B., A.T. Greenfield, P. Svenningsson, D.C. Haspeslagh, and P. Greengard. 2004. Phactrs 1-4: A family of protein phosphatase 1 and actin regulatory proteins. *Proc. Natl. Acad. Sci. USA.* 101:7187-92.
- Bañuelos, S., M. Saraste, and K. Djinović Carugo. 1998. Structural comparisons of calponin homology domains: implications for actin binding. *Structure.* 6:1419-31.
- Batchelor, C.L., A.M. Woodward, and D.H. Crouch. 2004. Nuclear ERM ezrin, radixin, moesin, proteins: regulation by cell density and nuclear import. *Exp. Cell Res.* 296:208-222.
- Bialkowska, K., T.C. Saido, and J.E. Fox. 2005. SH3 domain of spectrin participates in the activation of Rac in specialized calpain-induced integrin signaling complexes. *J. Cell Sci.* 118:381-395.
- Brown, E.J., J.S. Schlöndorff, D.J. Becker, H. Tsukaguchi, A.L. Uscinski, H.N. Higgs, J.M. Henderson, M.R. Pollak, and S.J. Tonna. 2010. Mutations in the formin gene INF2 cause focal segmental glomerulosclerosis. *Nat. Genet.* 421:72-6.
- Campellone, K.G., N.J. Webb, E.A. Znameroski, and M.D. Welch. 2008. WHAMM is an Arp2/3 complex activator that binds microtubules and functions in ER to Golgi transport. *Cell.* 134:148-61.

- Chakkalakal, J.V., M.A. Stocksley, M.A. Harrison, L.M. Angus, J. Deschenes-Furry, S. St-Pierre, L.A. Megeney, E.R. Chin, R.N. Michel, and B.J. Jasmin. 2003. Expression of utrophin A mRNA correlates with the oxidative capacity of skeletal muscle fiber types and is regulated by calcineurin/NFAT signaling. *Proc. Natl. Acad. Sci. USA.* 100(13):7791-6.
- Chereau, D., F. Kerff, P. Graceffa, Z. Grabarek, K. Langsetmo, and R. Dominguez. 2005. Actin-bound structures of Wiskott-Aldrich syndrome protein (WASP)-homology domain 2 and the implications for filament assembly. *Proc. Natl. Acad. Sci. USA.* 102:16644-9.
- Chhabra, E.S. and H.N. Higgs. 2006. INF2 Is a WASP homology 2 motif-containing formin that severs actin filaments and accelerates both polymerization and depolymerization. *J. Biol. Chem.* 281(36):26754-67.
- Chishti, A.H., et al. 1998. The FERM domain: a unique module involved in the linkage of cytoplasmic proteins to the membrane. *Trends Biochem. Sci.* 23:281-2.
- Dettenhofer, M., F. Zhou, and P. Leder. 2008. Formin 1-isoform IV deficient cells exhibit defects in cell spreading and focal adhesion formation. *PLoS One.* 36:e2497.
- Djinovic-Carugo K., P. Young, M. Gautel, and M. Saraste. 1999. Structure of the alpha-actinin rod: molecular basis for cross-linking of actin filaments. *Cell.* 98:537-546.
- Egile, C., T.P. Loisel, V. Laurent, R. Li, D. Pantaloni, P.J. Sansonetti, and M.F. Carlier. 1999. Activation of the CDC42 effector N-WASP by the Shigella

- flexneri IcsA protein promotes actin nucleation by Arp2/3 complex and bacterial actin-based motility. *J Cell Biol.* 1466:1319-32.
- Fehon, R.G., A.I. McClatchey, and A. Bretscher. 2010. Organizing the cell cortex: the role of ERM proteins. *Nat. Rev. Mol. Cell. Biol.* 11:276-87.
- Fontao, L., D. Geerts, I. Kuikman, J. Koster, D. Kramer, and A. Sonnenberg. 2001. The interaction of plectin with actin: evidence for cross-linking of actin filaments by dimerization of the actin-binding domain of plectin. *J Cell Sci.* 11:2065-76.
- Frazier, J.A., and C.M. Field. 1997. Actin cytoskeleton: are FH proteins local organizers? *Curr. Biol.* 7:R414-7.
- González, E., C. Montañez, P.N. Ray, P.L Howard, F. García-Sierra, D. Mornet, and B. Cisneros. 2000. Alternative splicing regulates the nuclear or cytoplasmic localization of dystrophin Dp71. *FEBS Lett.* 4823:209-14.
- Grosshans, J., C. Wenzl, H.M. Herz, S. Bartoszewski, F. Schnorrer, N. Vogt, H. Schwarz, and H.A. Müller. 2005. RhoGEF2 and the formin Dia control the formation of the furrow canal by directed actin assembly during Drosophila cellularisation. *Development.* 132:1009-20.
- Habas, R., Y. Kato, and X. He. 2001. Wnt/Frizzled activation of Rho regulates vertebrate gastrulation and requires a novel Formin homology protein Daam1. *Cell.* 107:843-854.
- Hemmings, L., D.J. Rees, V. Ohanian, S.J. Bolton, A.P. Gilmore, B. Patel, H. Priddle, J.E. Trevithick, R.O. Hynes, and D.R. Critchley. 1996. Talin

- contains three actin-binding sites each of which is adjacent to a vinculin-binding site. *J. Cell Sci.* 109:2715-26.
- Higgs, H.N. 2005. Formin proteins: a domain-based approach. *Trends Biochem Sci.* 30:342-53.
- Hotulainen, P., and P. Lappalainen. 2006. Stress fibers are generated by two distinct actin assembly mechanisms in motile cells. *J. Cell Biol.* 173:383-94.
- Ishiguro, H., T. Shimokawa, T. Tsunoda, T. Tanaka, Y. Fujii, Y. Nakamura, and Y. Furukawa. 2002. Isolation of HELAD1, a novel human helicase gene up-regulated in colorectal carcinomas. *Oncogene.* 21:6387-6394.
- Ishisaki Z., M. Takaishi, I. Furuta, and N. Huh. 2001. Calmin, a protein with calponin homology and transmembrane domains expressed in maturing spermatogenic cells. *Genomics.* 74:172-179.
- Karinch, A.M., W.E. Zimmer, and S.R. Goodman. 1990. The identification and sequence of the actin-binding domain of human red blood cell beta-spectrin. *J. Biol. Chem.* 26520:11833-40.
- Kobielska, A., H.A. Pasolli, and E. Fuchs. 2004. Mammalian formin-1 participates in adherens junctions and polymerization of linear actin cables. *Nat. Cell Biol.* 61:21-30.
- Lebensohn, A.M. and M.W. Kirschner. 2009. Activation of the WAVE complex by coincident signals controls actin assembly. *Mol Cell.* 36:512-24.
- Leung, C.L., D. Sun, M. Zheng, D.R. Knowles, and R.K. Liem. 1999. Microtubule actin cross-linking factor MACF: a hybrid of dystonin and dystrophin that

- can interact with the actin and microtubule cytoskeletons. *J. Cell Biol.* 1476:1275-86.
- Lu, J., W. Meng, F. Poy, S. Maiti, B.L. Goode, and M.J. Eck. 2007. Structure of the FH2 domain of Daam1: implications for formin regulation of actin assembly. *J Mol Biol.* 369:1258-69.
- Machesky, L.M., R.D. Mullins, H.N. Higgs, D.A. Kaiser, L. Blanchoin, R.C. May, M.E. Hall, and T.D. Pollard. 1999. Scar, a WASp-related protein, activates nucleation of actin filaments by the Arp2/3 complex. *Proc. Natl. Acad. Sci. USA.* 96:3739-44.
- McCann, R.O., and S.W. Craig. 1997. The I/LWEQ module: a conserved sequence that signifies F-actin binding in functionally diverse proteins from yeast to mammals. *Proc. Natl. Acad. Sci. USA.* 94:5679-84.
- Metzler, M., V. Legendre-Guillemain, L. Gan, V. Chopra, A. Kwok, P.S. McPherson, and M.R. Hayden. 2001. HIP1 functions in clathrin-mediated endocytosis through binding to clathrin and adaptor protein 2. *J. Biol. Chem.* 276:39271-6.
- Mills, I.G., L. Gaughan, C. Robson, T. Ross, S. McCracken, J. Kelly, and D.E. Neal. 2005. Huntington interacting protein 1 modulates the transcriptional activity of nuclear hormone receptors. *J. Cell Biol.* 170:191-200.
- Moores, C.A., N.H. Keep, and J. Kendrick-Jones. 2000. Structure of the utrophin actin-binding domain bound to F-actin reveals binding by an induced fit mechanism. *J. Mol. Biol.* 297:465-80.

- Panchal, S.C., D.A. Kaiser, E. Torres, T.D. Pollard, and M.K. Rosen. 2003. A conserved amphipathic helix in WASP/Scar proteins is essential for activation of Arp2/3 complex. *Nat. Struct. Biol.* 10:591-8.
- Rybakova, I.N., K.J. Amann, and J.M. Ervasti. 1996. A new model for the interaction of dystrophin with F-actin. *J. Cell Biol.* 1353:661-72.
- Saleh, H.S., U. Merkel, K.J. Geissler, T. Sperka, A. Sechi, C. Breithaupt, and H. Morrison. 2009. Properties of an ezrin mutant defective in F-actin binding. *J. Mol. Biol.* 385:1015-31.
- Schmidt, K.L., N. Marcus-Gueret, A. Adeleye, J. Webber, D. Baillie, and E.G. Stringham. 2009. The cell migration molecule UNC-53/NAV2 is linked to the ARP2/3 complex by ABI-1. *Development*. 136:563-74.
- Schultz, J., R.R. Copley, T. Doerks, C.P. Ponting, and P. Bork. 2000. SMART: a web-based tool for the study of genetically mobile domains. *Nucleic Acids Res.* 28:231-4.
- Shimada, A., M. Nyitrai, I.R. Vetter, D. Kühlmann, B. Bugyi, S. Narumiya, M.A. Geeves, and A. Wittinghofer. 2004. The core FH2 domain of diaphanous-related formins is an elongated actin binding protein that inhibits polymerization. *Mol. Cell.* 13:511-22.
- Sigrist, C.J.A., L. Cerutti, N. Hulo, A. Gattiker, L. Falquet, M. Pagni, A. Bairoch, and P. Bucher. 2002. PROSITE: a documented database using patterns and profiles as motif descriptors. *Brief Bioinformatics*. 3:265-74.
- Taniguchi, K., R. Takeya, S. Suetsugu, M. Kan-O, M. Narusawa, A. Shiose, R. Tominaga, and H. Sumimoto. 2009. Mammalian formin fhod3 regulates

- actin assembly and sarcomere organization in striated muscles. *J. Biol. Chem.* 284, 29873-81.
- Tidball, J.G. and M.J. Spencer. 1993. PDGF Stimulation Induces Phosphorylation of Talin and Cytoskeletal Reorganization in Skeletal Muscle. *J. Cell Biol.* 123, 627-635.
- Vidali, L., P.A. van Gisbergen, C. Guérin, P. Franco, M. Li, G.M. Burkart, R.C. Augustine, L. Blanchoin, and M. Bezanilla. 2009. Rapid formin-mediated actin-filament elongation is essential for polarized plant cell growth. *Proc. Natl. Acad. Sci. USA.* 10632:13341-6.
- Wilbur, J.D., C.Y. Chen, V. Manalo, P.K. Hwang, R.J. Fletterick, and F.M. Brodsky. 2008. Actin binding by Hip1 huntingtin-interacting protein 1. and Hip1R Hip1-related protein. is regulated by clathrin light chain. *J. Biol. Chem.* 283:32870-9.
- Winder, S.J., L. Hemmings, S.K. Maciver, S.J. Bolton, J.M. Tinsley, K.E. Davies, D.R. Critchley, and J. Kendrick-Jones. 1995. Utrophin actin binding domain: analysis of actin binding and cellular targeting. *J. Cell Sci.* 108(Pt 1):63-71.
- Wu, X., Y. Yoo, N. Okuhama, P. Tucker, G. Liu, and J. Guan. 2006. Regulation of RNA-polymerase-II-dependent transcription by N-WASP and its nuclear-binding partners. *Nat. Cell Biol.* 8:756-63.
- Wu, X., A. Kodama, and E. Fuchs. 2008. ACF7 regulates cytoskeletal-focal adhesion dynamics and migration and has ATPase activity. *Cell.* 1351:137-48.

- Yamashiro-Matsumura S and F. Matsumura. 1986. Intracellular localization of the 55-kD actin-bundling protein in cultured cells: spatial relationships with actin, alpha-actinin, tropomyosin, and fimbrin. *J. Cell Biol.* 1032:631-40.
- Young, K.G., M. Pool, and R. Kothary. 2003. Bpag1 localization to actin filaments and to the nucleus is regulated by its N-terminus. *J. Cell Sci.* 116:4543-55.
- Young, K.G. and R. Kothary. 2008. Dystonin/Bpag1 is a necessary endoplasmic reticulum/nuclear envelope protein in sensory neurons. *Exp. Cell Res.* 314:2750-2761.
- Zernig, G. and G. Wiche. 1985. Morphological integrity of single adult cardiac myocytes isolated by collagenase treatment: immunolocalization of tubulin, microtubule-associated proteins 1 and 2, plectin, vimentin, and vinculin. *Eur. J. Cell Biol.* 381:113-22.
- Zhang, Q., C. Ragnauth, M.J. Greener, C.M. Shanahan, and R.G. Roberts. 2002. The nesprins are giant actin-binding proteins, orthologous to *Drosophila melanogaster* muscle protein MSP-300. *Genomics*. 80:473-481.
- Zhang, Q., C, et al. 2007. Nesprin-1 and -2 are involved in the pathogenesis of Emery Dreifuss muscular dystrophy and are critical for nuclear envelope integrity. *Hum. Mol. Genet.* 1623:2816-33.

Zuchero, Belin, and Mullins
Table S1

Gene	UniProt	ABD	Loc.	Function	References
ACTN2	P35609	CH	cyt, nuc [‡]	cytoskeletal linker	(Yamashiro-Matsumura and Matsumura, 1986) (Djinovic-Carugo et al., 1999)
CLMN	Q96JQ2	CH	cyt, nuc [‡]	unknown	(Ishisaki et al., 2001)
COBL	O75128	WH2	cyt, nuc	actin nucleator	(Ahuja et al., 2007)
DAAM1, 2	Q9Y4D1, Q86T65	FH2	cyt, nuc	formin actin nucleator	(Habas et al., 2001) (Lu et al., 2007)
DIAPH1	O60610	FH2	cyt, nuc	formin actin nucleator	(Grosshans et al., 2005) (Hotulainen and Lappalainen, 2006)
DMD	P11532	CH	cyt, nuc [‡]	cytoskeletal linker	(Rybakova et al., 1996) (González et al., 2000)
DST	Q03001	CH	cyt, nuc	cytoskeletal linker	(Young et al., 2003) (Young and Kothary, 2008)
EZR/RDX /MSN	P15311, P35241	ERM	cyt, nuc	cytoskeletal linker, focal adhesions	(Batchelor et al., 2004) (Fehon et al., 2010)
FHOD3	Q2V2M9	FH2	cyt	formin actin nucleator	(Taniguchi et al., 2009)
FMN1	Q68DA7	FH2	cyt	formin actin nucleator	(Kobielak et al., 2004) (Dettenhofer et al., 2008)
FMNL2	Q96PY5	FH2	cyt, nuc [‡]	formin actin nucleator	(Vidali et al., 2009)
HIP1	O00291	ERM, I/LWEQ	cyt, nuc [‡]	endocytosis	(Metzler et al., 2001) (Mills et al., 2005) (Wilbur et al., 2008)
INF2	Q27J81	FH2	cyt, nuc [‡]	formin actin nucleator	(Chhabra and Higgs, 2006) (Brown et al., 2010)
JMY	Q8N9B5	WH2	cyt, nuc	actin nucleator, transcription	(Shikama et al., 1999) (Zuchero et al., 2009)
MACF1	Q9UPN3	CH	cyt	cytoskeletal linker	(Leung et al., 1999) (Wu et al., 2008)
MAL (MKL1)	Q969V6	RPEL	cyt, nuc	transcription	(Miralles et al., 2003) (Vartiainen et al., 2007)
NAV2	Q8IVL1	CH, I/LWEQ*	cyt, nuc [‡]	cell migration	(Ishiguro et al., 2002) (Schmidt et al., 2009)
PHACTR 1-4	Q9C0D0, Q8IZ21	RPEL	cyt, nuc	unknown	(Sagara et al., 2003) (Allen et al., 2004)
PLEC1	Q15149	CH	cyt	cytoskeletal linker	(Zernig and Wiche, 1985) (Fontao et al., 2001)
SPIR1	Q08AE8	WH2	cyt	actin nucleator	(Quinlan et al., 2005)
SPTB1	P11277	CH	cyt, nuc	cytoskeletal linker, plasma and inner nuclear membrane	(Karinch et al., 1990) (Bialkowska et al., 2005)
SYNE1	Q8NF91	CH	cyt, nuc	cytoskeletal linker, nuclear	(Zhang et al., 2002) (Zhang et al., 2007)

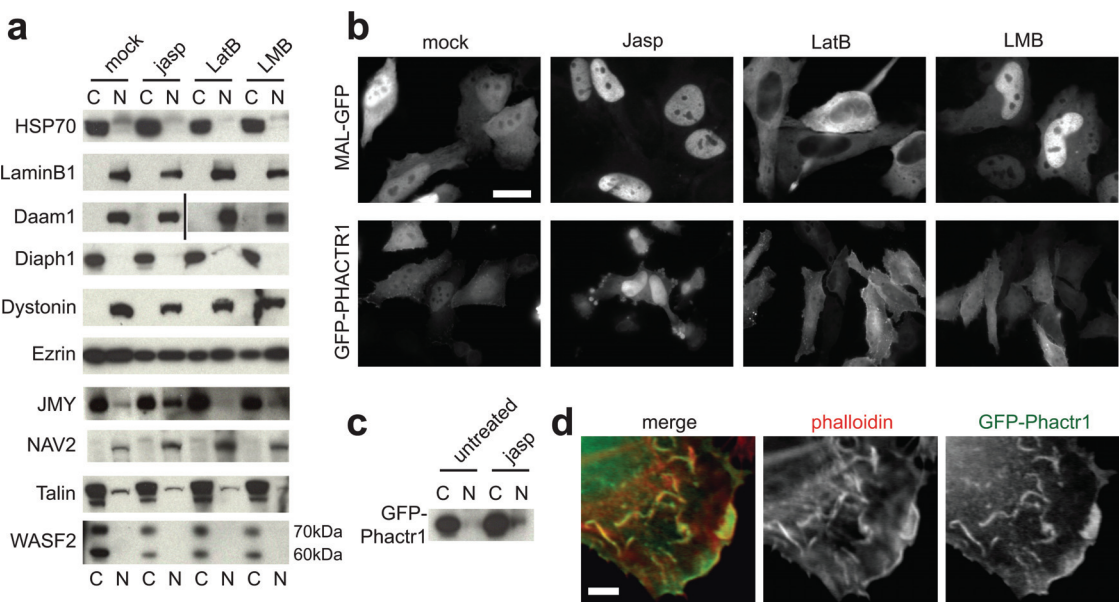
				membrane	
TLN1	Q9Y490	ERM, I/LWEQ	cyt [‡]	cytoskeletal linker, focal adhesions	(Tidball and Spencer, 1993) (Hemmings et al., 1996)
UTRO	P46939	CH	cyt	cytoskeletal linker	(Winder et al., 1995) (Chakkalakal et al., 2003)
WASF2, 4	Q9Y6W5, Q8IV90	WH2*	cyt	Arp2/3 activator	(Machesky et al., 1999) (Lebensohn and Kirschner, 2009)
WASL	O00401	WH2	cyt, nuc	Arp2/3 activator	(Egile et al., 1999) (Wu et al., 2006)

Supplemental Table and Figure Legends

Supplemental Table S1. Expanded version of table from Fig. 1A, of all high confidence hits containing both a putative NLS and ABD. Table shows gene name, Uniprot number (<http://www.uniprot.org>), actin binding domain (ABD), localization (Loc.), cellular function, and references. Actin monomer-binding or filament-binding domains were identified using the NCBI BLASTp search tool, based on detectable similarity (evalue<0.05) to consensus sequences built from published sequences (see Supplementary Methods). Bold shows genes in which there is overlap between NLS and ABD (see also Fig. 1A). * denotes putative (uncharacterized) ABDs. ‡, Localization based on micrographs from the Human Protein Atlas (<http://www.proteinatlas.org>).

Abbreviations used in table: ACTN2, Alpha-actinin 2; CLMN, Calmin; COBL, Cordon-bleu; DAAM, Disheveled-associated activator of morphogenesis 1; DIAPH1, Diaphanous homolog 1; DMD, Dystrophin; DST, Dystonin (Bullous pemphigoid antigen 1); EZR, Ezrin; RDX, Radixin; MSN, Moesin; FHOD3, Formin Homology Domain containing 3; FMN1, Formin 1; FMNL2, Formin-like 2; HIP1, Huntingtin-interacting protein 1; INF2, Inverted Formin 2; JMY, Junction-

mediating and regulatory protein; MACF1, Microtubule-Actin Cross-Linking Factor 1 (Actin Cross-Linking Factor 7); MAL (MKL1), Myocardin-like protein 1; NAV2, Neuron Navigator 2; PHACTR, Phosphatase and actin regulator; PLEC1, Plectin; SPIR1, Spire; SPTB1, Beta-Spectrin; SYNE1, Nesprin-1 (SYNE1); TLN1, Talin 1; UTRO, Utrophin; WASF2, WASP-family 2 (WAVE2); WASL, N-WASP. Actin binding domains are: FH2, Formin Homology 2 domain; CH, Calponin Homolgy domain; ERM, Ezrin/Radixin/Moesin domain; WH2, Wiscott-Aldrich Homology 2 domain.



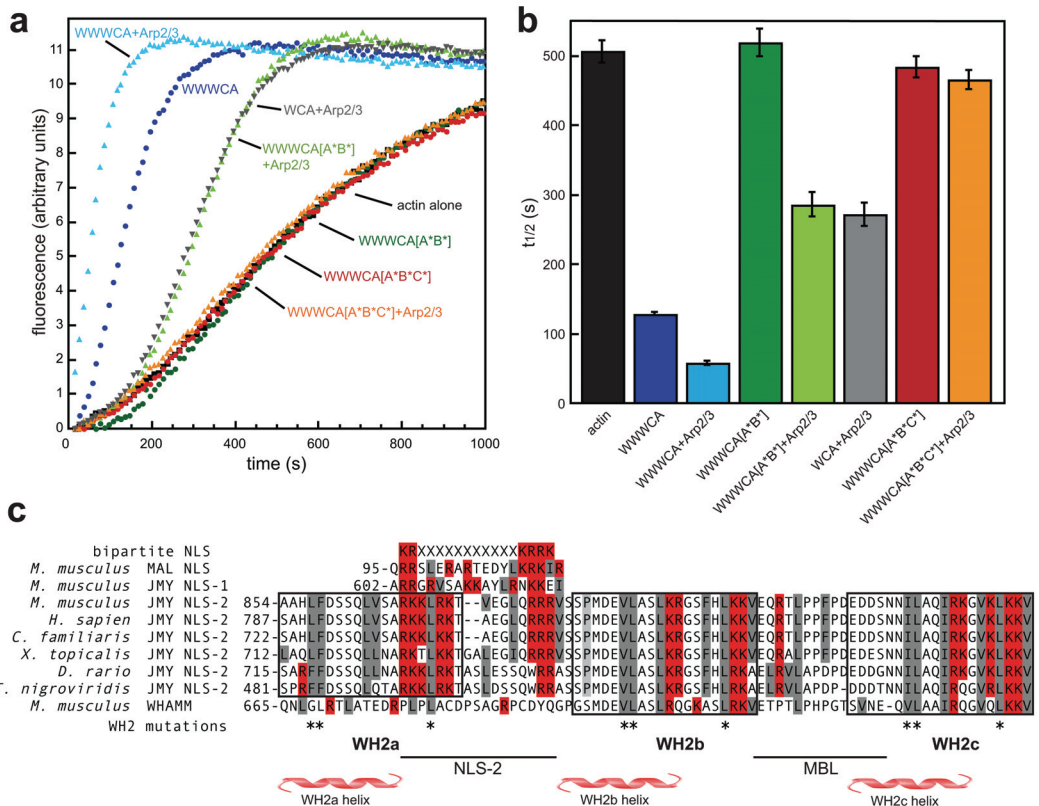
Supplemental Figure S1.

(A) Fractionation of endogenous proteins from cells treated with either 500 nM jasplakinolide (jasp), 500 nM Latrunculin B (LatB), or 20 nM Leptomycin B (LMB) for 30 minutes. (See Methods.)

(B) MAL-GFP shuttles between the nucleus and cytoplasm in an actin- and CRM1-dependent manner (top panels). GFP-Phactr1 modestly accumulates in the nucleus after polymerization of actin with jasp (bottom panels). HeLa cells were transiently transfected with constructs, treated with 500 nM jasp or LatB, or 20 nM LMB as indicated, then fixed and imaged. Scale bar, 20 μm .

(C) Analysis of jasp-induced GFP-Phactr1 nuclear accumulation. GFP-Phactr1 was transiently expressed in HeLa cells as above, treated with 500 nM jasp where noted, then fractionated into cytoplasmic and nuclear pools. Immunoblots using an anti-GFP antibody demonstrate that some GFP-Phactr1 is found in the nuclear fraction after treatment with jasp.

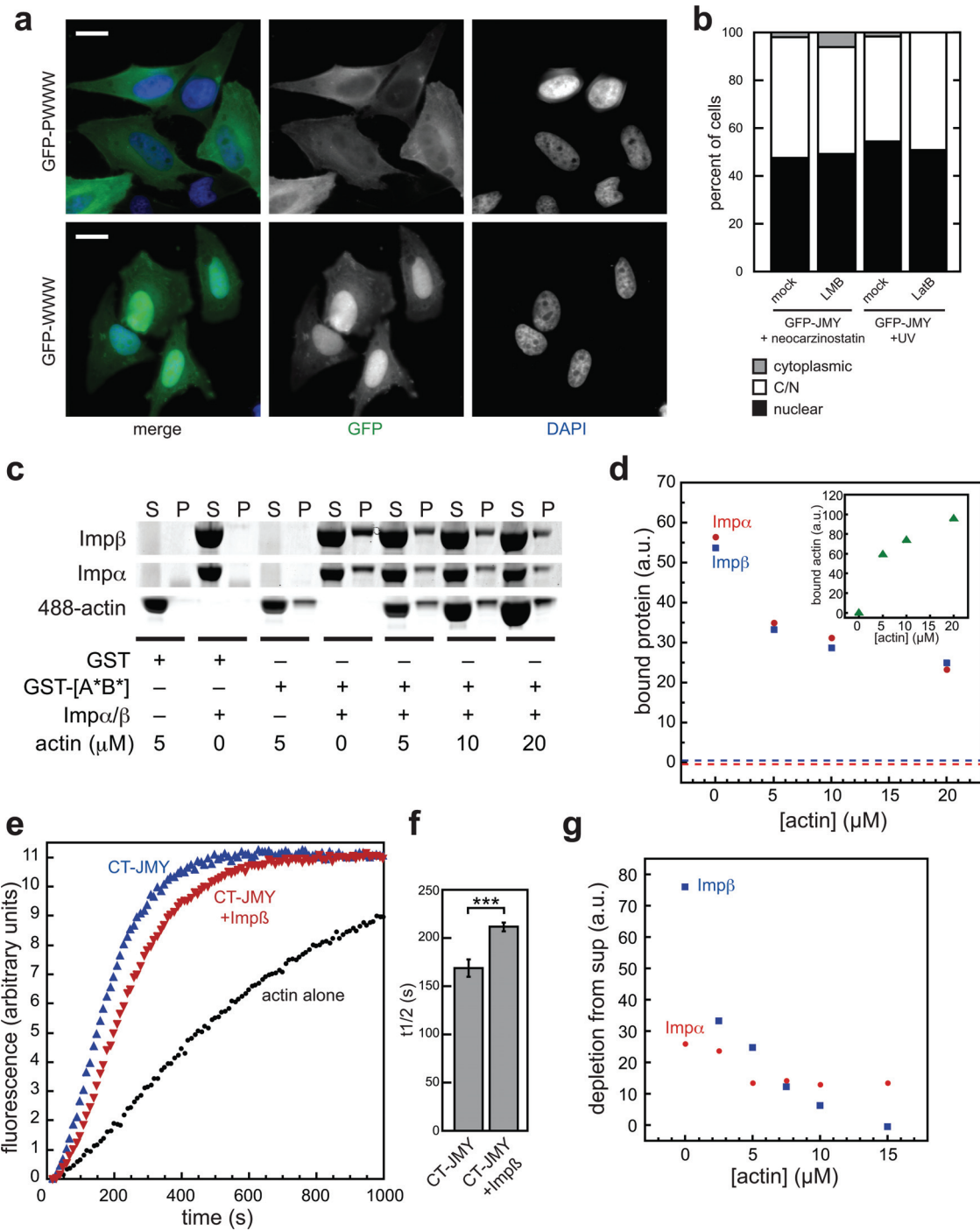
(D) GFP-Phactr1 (green) colocalizes with actin filament structures (red) in HeLa cells. Scale bar, 5 μm .



Supplemental Figure S2.

(A-B) JMY WH2 point mutations compromise actin binding. Mutating WH2a and WH2b; (WWWCA[A*B*]) blocks nucleation but allows activation of the Arp2/3 complex, with the same kinetics as WCA. Mutating all three WH2 domains (WWWCA[A*B*C*]) blocks both nucleation and activation. (B) Quantification of average time to half-maximal fluorescence ($t^{1/2}$) for each reaction. Error bars, s.e.m.

(C) Sequence alignment of JMY WWW region. NLS-2 and the monomer binding linker (MBL) are underlined. Alignment includes JMY NLS-1, MAL NLS, and the classical SV40 large T-antigen NLS. WH2 mutations are indicated with asterisks, and the position of the putative alpha helical regions of JMY WH2 domains are indicated with helix cartoons. Note that NLS-2 is not conserved in the closely related protein WHAMM (Campellone et al., 2008).



Supplemental Figure S3.

(A) GFP-PWWW (top) is cytoplasmic, but GFP-WWW (bottom) is nuclear, suggesting that polyproline domain is required for actin to bind to WH2s. See

also quantification in Fig. 2F. HeLa cells were transiently transfected with constructs, grown for 48 hr, then fixed and imaged. Scale bars, 20 μ m.

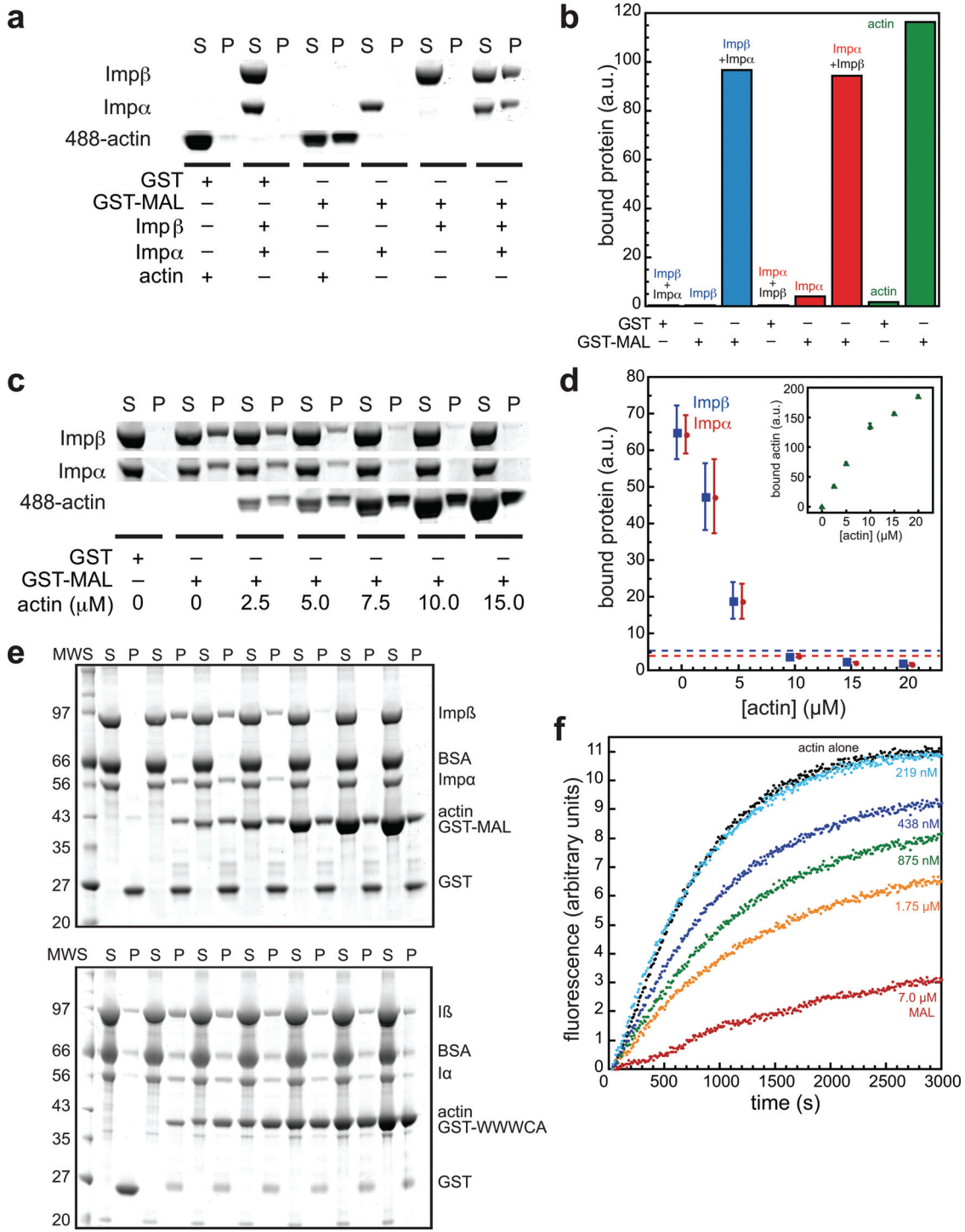
(B) UV-induced DNA damage (50 J/m²) was used to redistribute GFP-JMY to the nucleus. Addition of LatB for 30 min to UV damaged cells (24 hr post-UV) has no significant effect.

(C-D) GST pulldown with JMY GST-WWWCA[A*B*] shows only a modest decrease in Importin binding, up to 20 μ M actin, at which point actin binding is saturated.

(E-F) Importin β (Imp β) modestly inhibits nucleation by CT-JMY. Pyrene actin polymerization assays were conducted with purified proteins (See Methods).

Time to half-maximal fluorescence ($t^{1/2}$) is plotted in E (***, p<0.005; n>3).

(G) Average depletion of Importin α (Imp α) and Imp β from the supernatant in pulldown assays shown in Figure 4, C and D. Depletion was calculated by subtracting supernatant band intensities from the intensity of supernatant collected from GST alone (control) beads. Graph shows the average of three independent experiments.



Supplemental Figure S4.

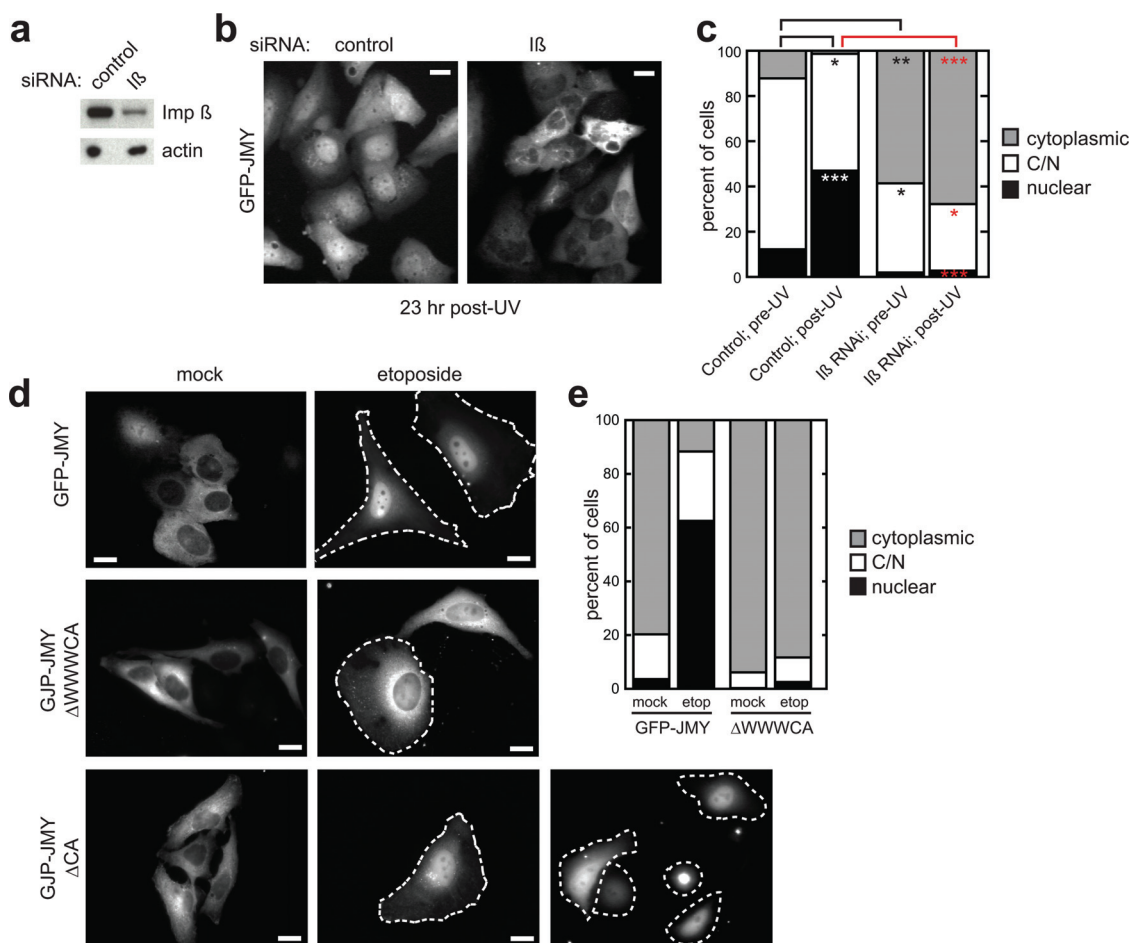
(A-B) GST pulldown showing that actin monomers, Imp α , and Imp β bind to MAL GST-RPEL cluster. GST-RPEL, bound to magnetic glutathione beads, was

incubated with purified proteins as in Fig. 4. Similar to classical NLS binding (but contrasting with binding to JMY) Imp α and Imp β only bind to MAL when both proteins are present. (A) SDS-PAGE gels were stained with Sypro Red to visualize proteins. (B) Bound proteins were quantified using ImageQuant software.

(C-D) Actin competes with Imp α/β for binding to MAL GST-RPEL cluster. GST-MAL beads were incubated with 2.5 μ M Imp α and Imp β and increasing concentrations of LatB-actin. In the presence of 10-15 μ M actin, Importin levels are indistinguishable from nonspecific binding. This occurs at a lower concentration than where actin binding saturates. (D) Quantification of bound Imp α and Imp β , showing the averages from three independent experiments. Inset shows bound actin. Error bars, s.e.m.

(E) Example gels from GST pulldown assays using GST-RPEL (top) and GST-JMY (bottom).

(F) Pyrene actin polymerization assays (see Methods) show that MAL does not nucleate actin, but inhibits spontaneous polymerization. At concentrations close to the concentration of actin, MAL sequesters monomers, evidenced by the decrease in rate of polymerization and total polymerization (plateau). At lower concentrations, MAL has no effect on actin assembly.



Supplemental Figure S5.

(A-C) Imp β is required for DNA damage-induced nuclear accumulation of GFP-JMY. Cells stably expressing GFP-JMY were transfected with siRNA, then grown for 72 hr prior to UV-irradiation (50 J/m²). (A) Immunoblotting shows that Imp β (top) expression was knocked down by Imp β -specific siRNA. Actin (bottom) was used as a loading control. (B) Following DNA damage GFP-JMY nuclear accumulation is greatly reduced in cells treated with Imp β siRNA, relative to control cells. (C) GFP-JMY localization was scored both before and 23 hr after UV damage, in cells treated with Imp β or control siRNA. >100 cells per condition,

n=3. *, p<0.05; **, p<0.01; ***, p<0.005. For t-tests, conditions are compared to control siRNA, pre-UV; except where indicated with the colored bracket.

(D-E) GFP-JMY (top), but not the truncation mutant Δ WWWCA (middle),

accumulates in the nucleus in response to DNA damage by etoposide.

Localization of the Δ CA truncation mutant is the same as full-length GFP-JMY

(bottom; two representative images of etoposide treatment are shown). JMY

constructs were transiently expressed in HeLa cells for 16 hr prior to treatment

with DMSO (mock; left panels) or 10 μ M etoposide (right panels) for 48 hr, then

fixed and imaged. (E) Quantification of >300 cells per condition, n \geq 2. C/N,

equally distributed in cytoplasm and nucleus.